A tömegspektrometria alapjai
Klinikai tömegspektrometriás vizsgálatok

Dr. Karvaly Gellért Balázs

Semmelweis Egyetem Laboratóriumi Medicina Intézet

Tömegspektrometriai és Elválasztástechnikai Laboratórium

Ion source	Mass analyzers
Electrospray ionization (ESI)	*Quadrupole*
Atmospheric pressure chemical ionization (APCI)	Ion trap
Atmospheric pressure photoionization (APPI)	Linear ion trap
Electron ionization	*Quadrupole-ion trap*
Chemical ionization	*Time of flight*
Nanospray ionization	Double focussing magnetic sector
Spark ionization	Radiofrequency mass analyzer
Thermospray ionization	Fourier transformation mass analyzer
Field ionization	Magnetic sector
Field desorption	Ion cyclotron resonance mass analyzer
Fast atom bombardment	Reversed geometry mass analyzer
Multiphoton ionization	Hybrid
Plasma desorption	Electronic sector
Laser desorption (MALDI, SELDI, infrared)	Orbitrap
Corona discharge ionization	

Mass ranges and sensitivities attainable using various ionization techniques

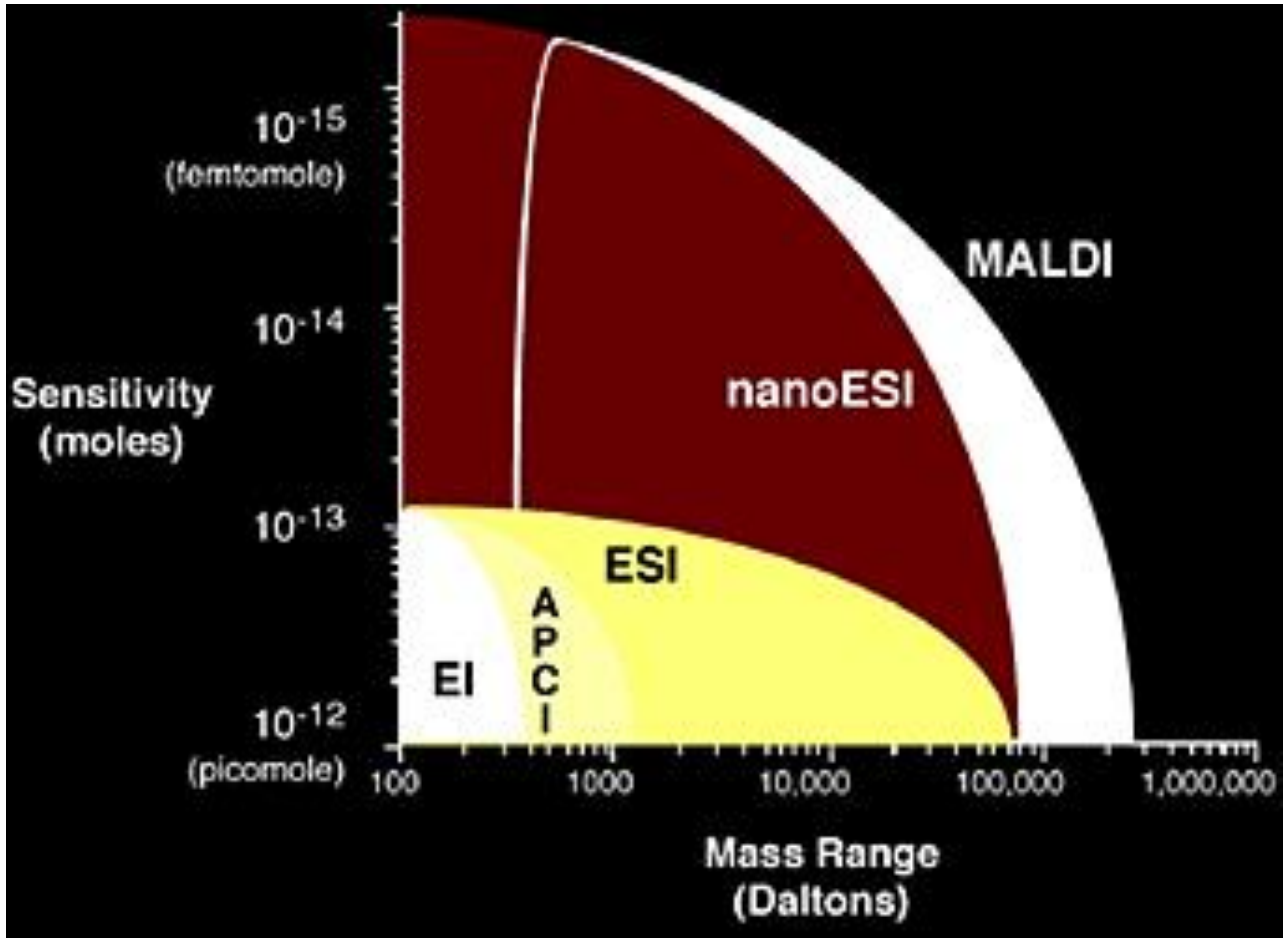

Electrospray ionization

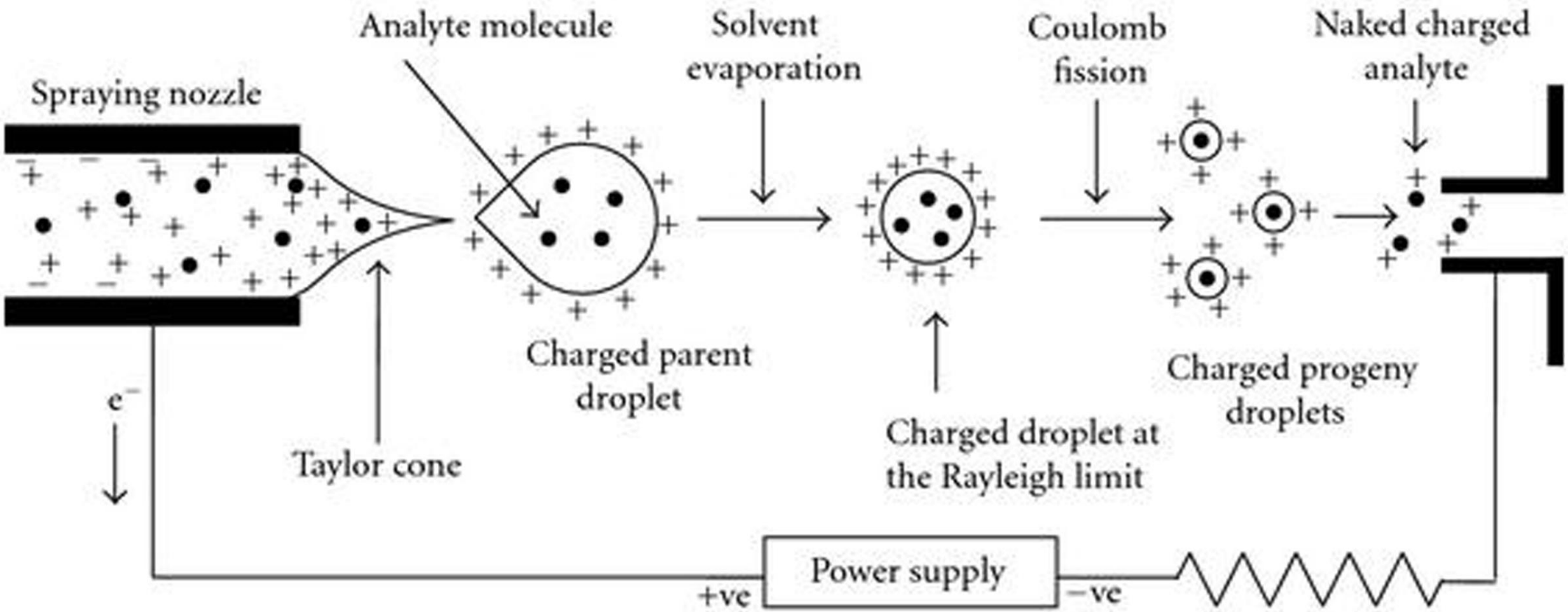

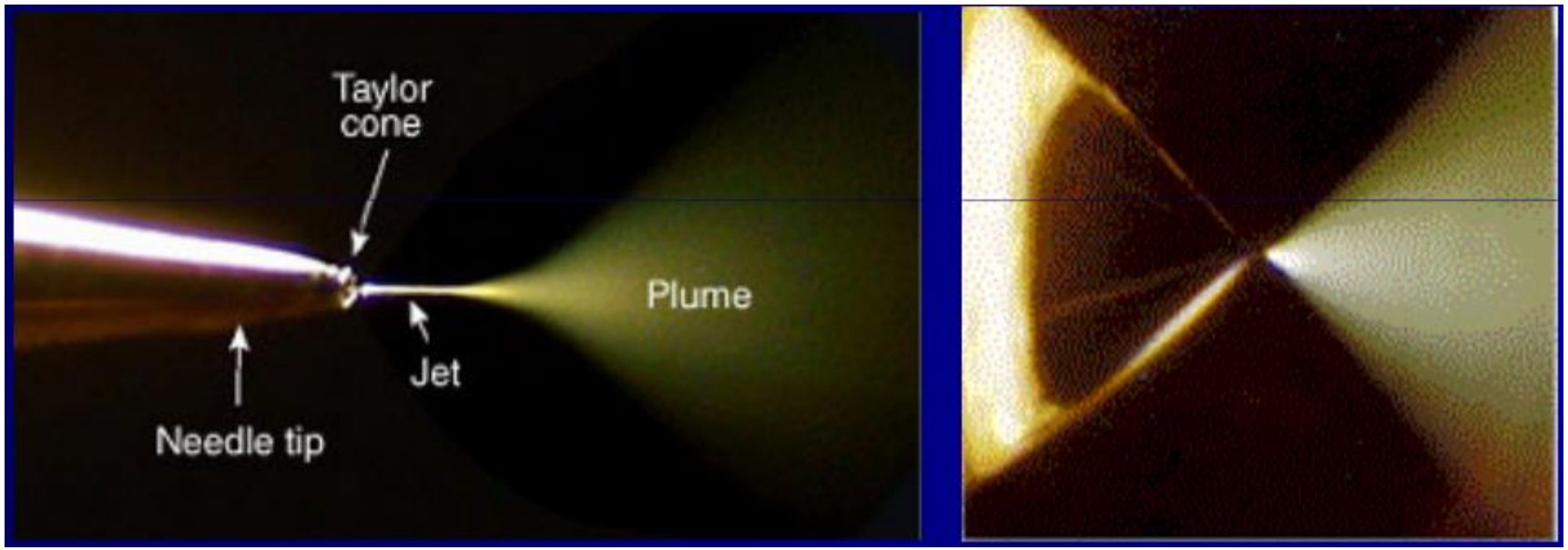
Taylor
cone
Plume
Jet
Needle tip

Simplified overview of the electrospray unit

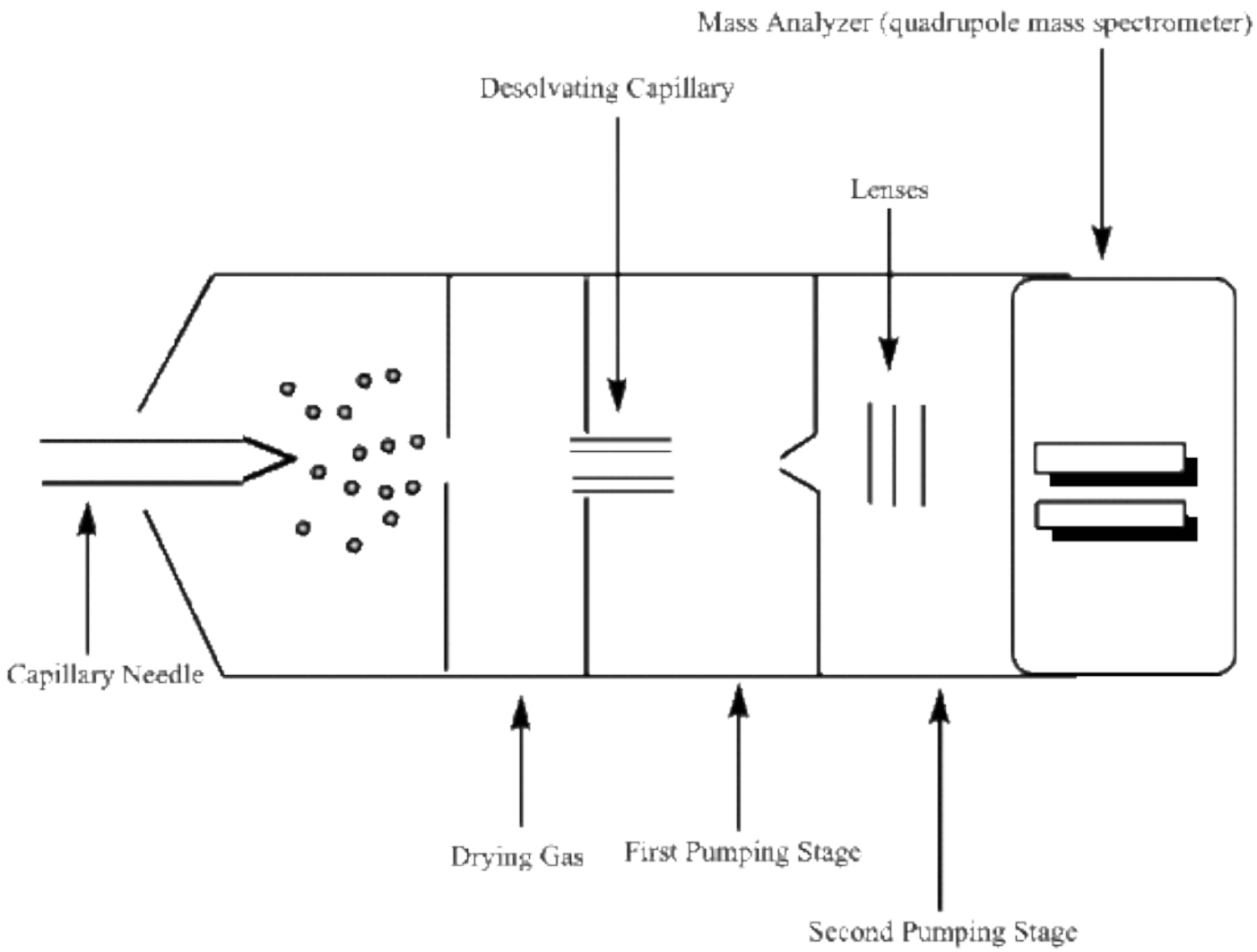

Formation of adducts during electrospray ionization

Observed	Explanation	Mass
$[M+H]^+$	Protonation	M+1
$[M-H]^-$	Deprotonation	M-1
$[M-H-nH_2O]^-$	Deprotonation and loss of H_2O	M-1-(nx18)
$[M+Cl]^-$	Ion attachment	M+35 (37)
$[M-2H+Na]^-$	M + Na adduct	M+21
$[M-H-CO_2]^-$	Carbon dioxide loss	M+45
$[M+H+CH_3CN]^+$	In presence of CH_3CN	M+42
$[M+H+CH_3CN+nH_2O]^+$	Water-acetonitrile cluster	M+42+(nx18)

Macromolecules have peak envelopes

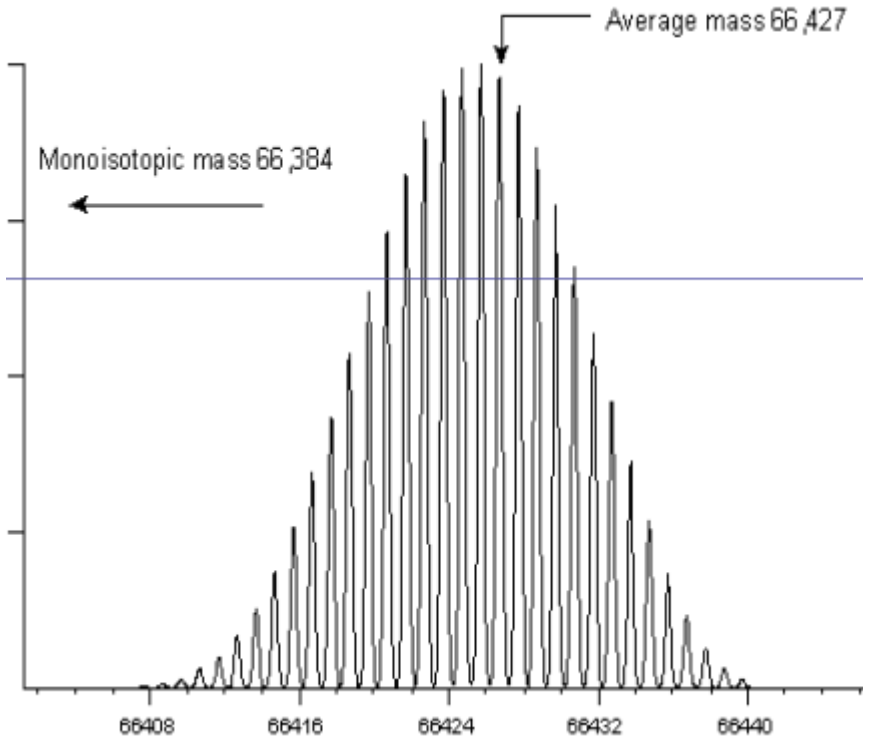

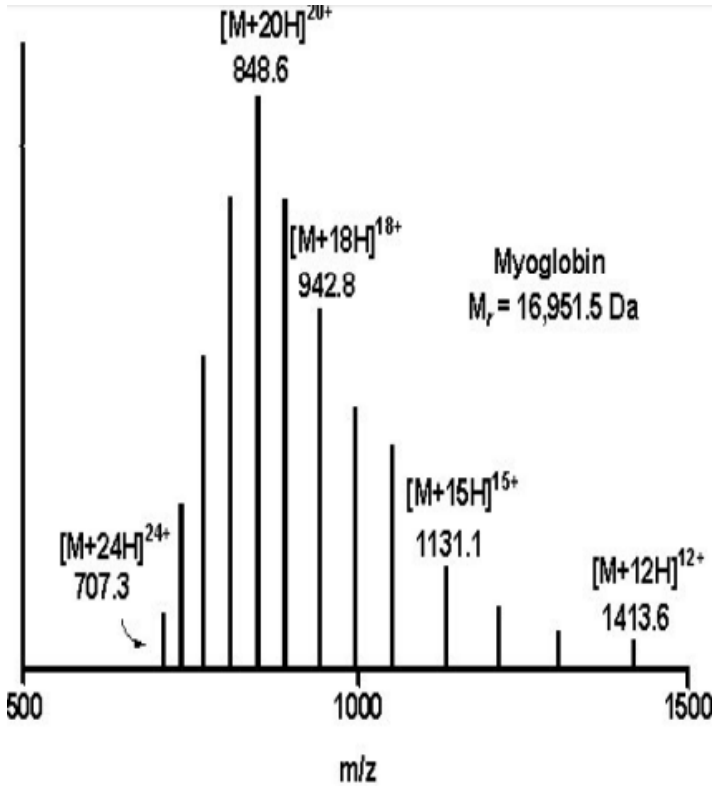

3% methanol

3% methanol

3% methanol

3% methanol

50% methanol

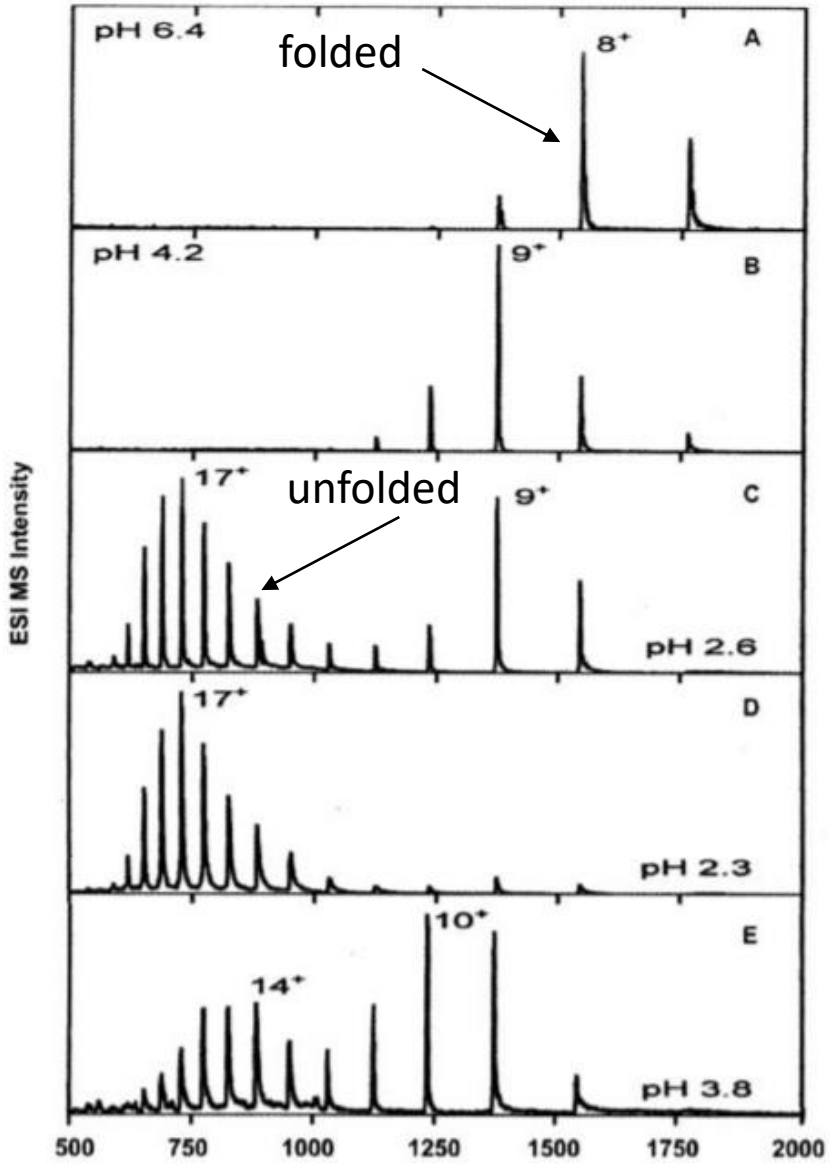

FIG. 3. **ESI mass spectra of cytochrome *c* in water containing 3% methanol and 0.5 mM ammonium acetate.** *A*, pH 6.4; *B*, pH 4.2; *C*, pH 2.6; *D*, pH 2.3; and *E*, in 50% methanol and 0.5 mM ammonium acetate at pH 3.8. (Reprinted with permission from Ref. 21.)

Native folded conformation, charge centered on +8 charge state

Native folded conformation, charge centered on +9 charge state

Yan X et al. Mol Cell Proteom 3 (2004), 10.

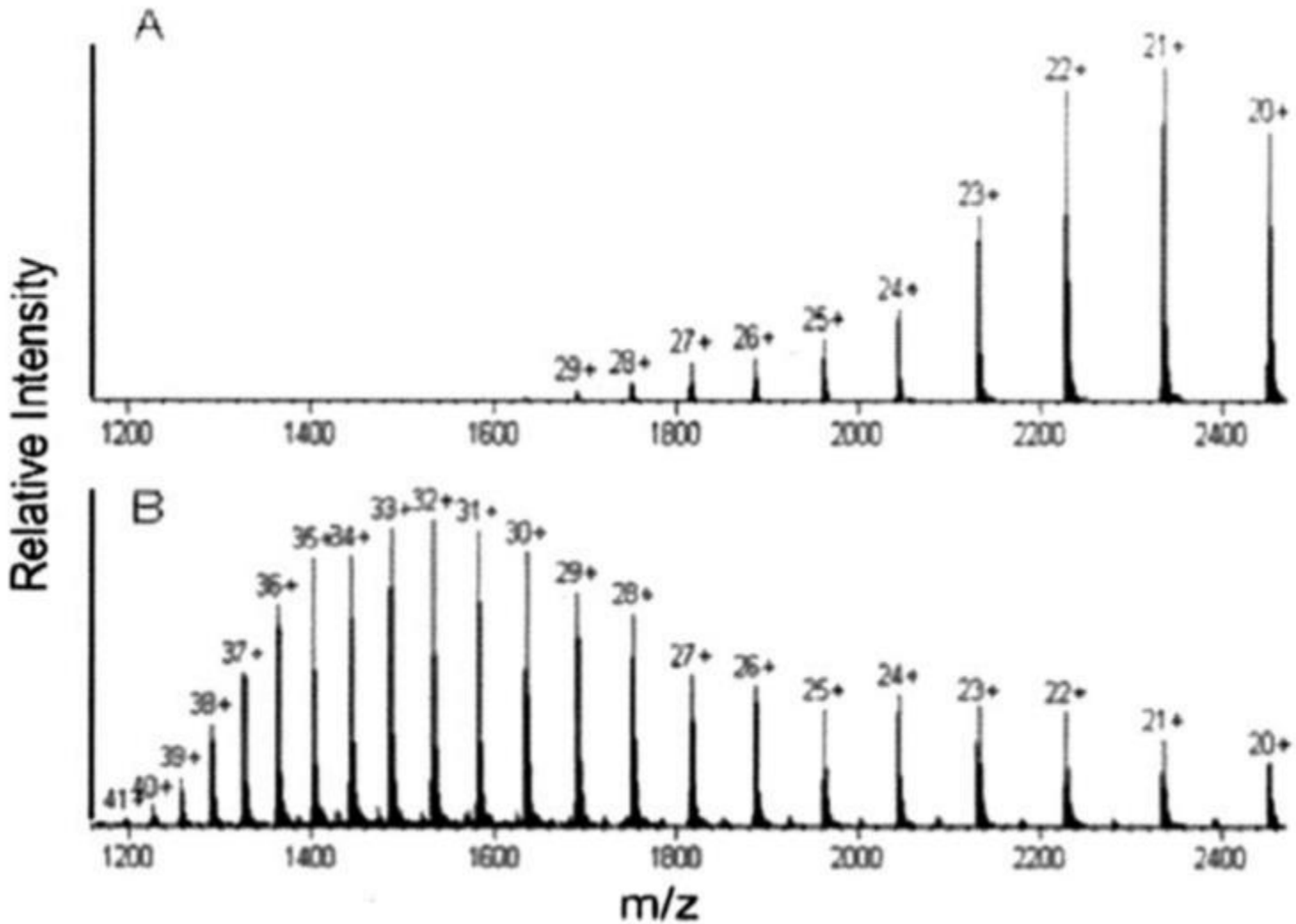

FIG. 4. **Positive ion ESI mass spectra of rhM-CSFβ sprayed from acetonitrile/H_2O containing 0.1% trifluoroacetic acid solution through a column.** *A*, Native state; and *B*, selectively reduced and blocked sulfhydryls C_{157}–C_{159}.

Yan X et al. Mol Cell Proteom 3 (2004), 10.

Matrix-assisted laser desorption ionization

MALDI-TOF has revolutionized the identification of microorganisms in clinical and public health laboratories

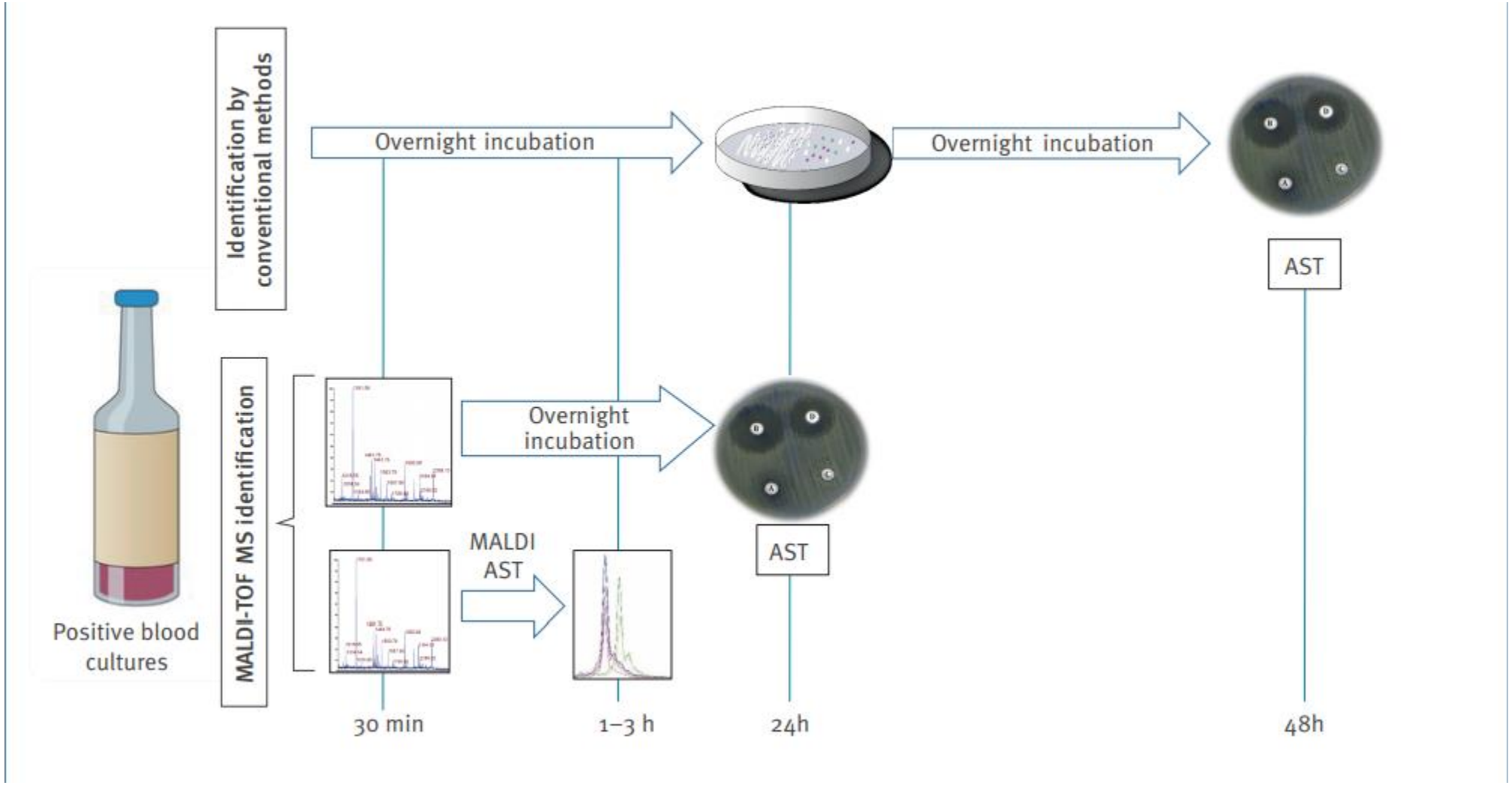

Rodríguez-Sánchez B et al. Euro Surveill 2019;24:pii=1800193.

Matrix-assisted laser desorption ionization

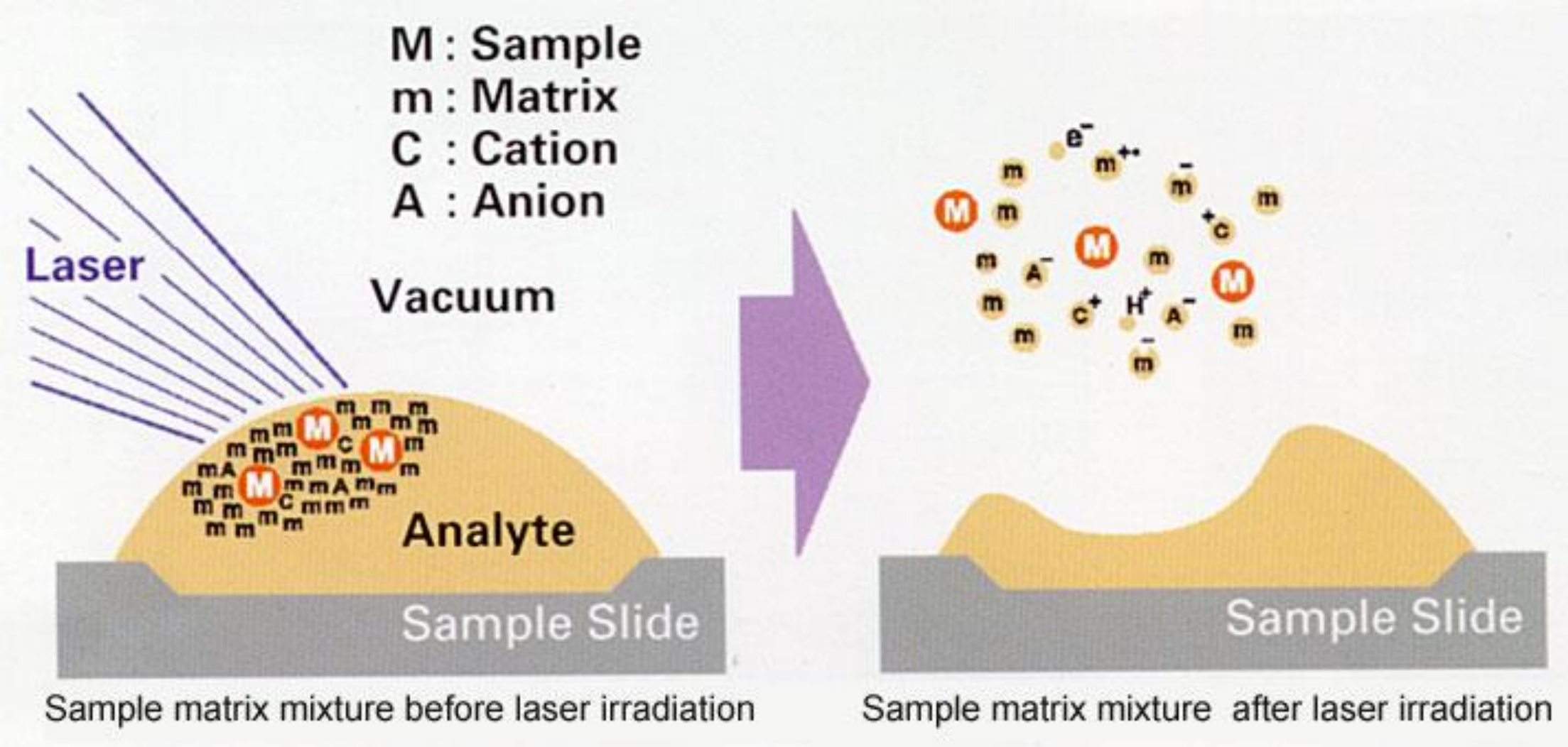

MALDI-TOF/TOF Mass Spectrometer

By Jeffrey M. Perkel

Perhaps no tool has been as instrumental to the proteomics revolution as the mass spectrometer. With the ability to deconvolute highly complex mixtures over a wide range of abundance levels, these machines enable researchers to identify and quantify proteins and to determine if and how those proteins have been post-translationally modified.

The basic mass spectrometer measures an ion's mass-to-charge (*m*/*z*) ratio only. This enables peptide mass fingerprinting, which is the identification of a protein based on the specific group of peptide masses it produces. But tandem devices, the so-called MS/MS instruments, can provide peptide sequence information as well. The key components shown on these pages demonstrate one of those instruments: the 4700 Proteomics Analyzer made by Applied Biosystems of Foster City, Calif., which features a MALDI (matrix-assisted laser desorption ionization) source and tandem time-of-flight (TOF/TOF) mass analyzers.

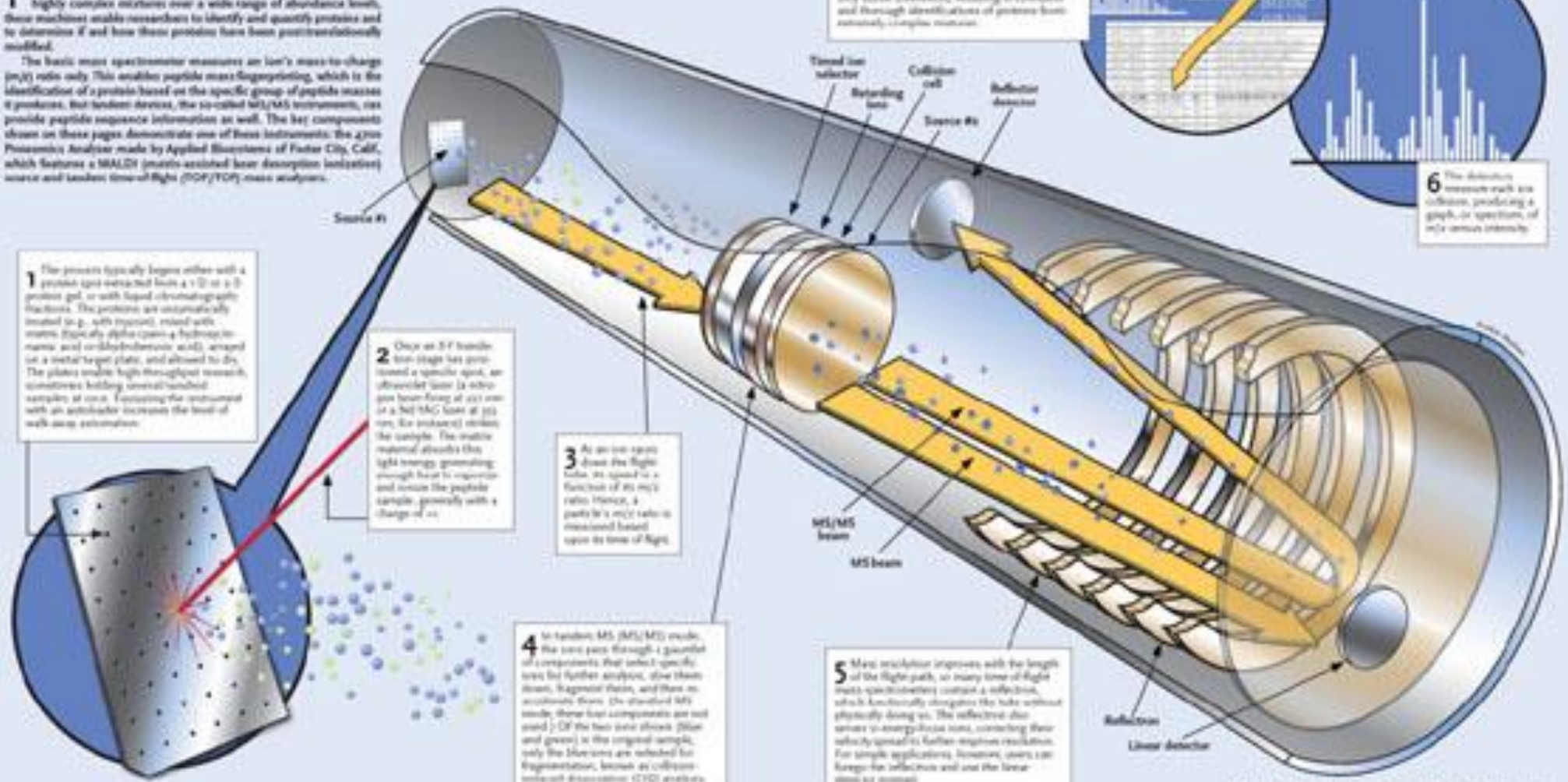

1 The process typically begins either with a protein spot extracted from a 1-D or a 2-D protein gel, or with liquid chromatography fractions. The proteins are enzymatically treated (e.g., with trypsin), mixed with matrix (typically alpha-cyano-4-hydroxycinnamic acid or dihydroxybenzoic acid), arrayed on a metal target plate, and allowed to dry. The plates enable high-throughput research, sometimes holding several hundred samples at once. Equipping the instrument with an autoloader increases the level of walk-away automation.

2 Once an X-Y translation stage has positioned a specific spot, an ultraviolet laser (a nitrogen laser firing at 337 nm or a Nd:YAG laser at 355 nm, for instance) strikes the sample. The matrix material absorbs this light energy, generating enough heat to vaporize and ionize the peptide sample, generally with a charge of +1.

3 As an ion races down the flight tube, its speed is a function of its *m*/*z* ratio. Hence, a particle's *m*/*z* ratio is measured based upon its time of flight.

4 In tandem MS (MS/MS) mode, the ions pass through a gauntlet of components that select specific ions for further analysis, slow them down, fragment them, and then accelerate them. (In standard MS mode, these four components are not used.) Of the two ions shown (blue and green) in the original sample, only the blue ions are selected for fragmentation, known as collision-induced dissociation (CID) analysis.

5 Mass resolution improves with the length of the flight path, so many time-of-flight mass spectrometers contain a reflectron, which functionally elongates the tube without physically doing so. The reflectron also serves to energy-focus ions, correcting their velocity spread to further improve resolution. For simple applications, however, users can forego the reflectron and use the linear detector instead.

6 The detector(s) measure each ion collision, producing a graph—or spectrum—of *m*/*z* versus intensity.

7 Comparing the resulting constellation of *m*/*z* values against a database identifies the peptide, and by extension, the protein from which it derives. Tandem MS/MS analysis of fragmented peptides produces an actual sequence, providing a more accurate protein ID. Today's mass spectrometers have high enough resolution and mass accuracy to distinguish peptides bearing only subtle differences, resulting in confident and thorough identifications of proteins from extremely complex mixtures.

Jeffrey M. Perkel can be contacted at jperkel@the-scientist.com.

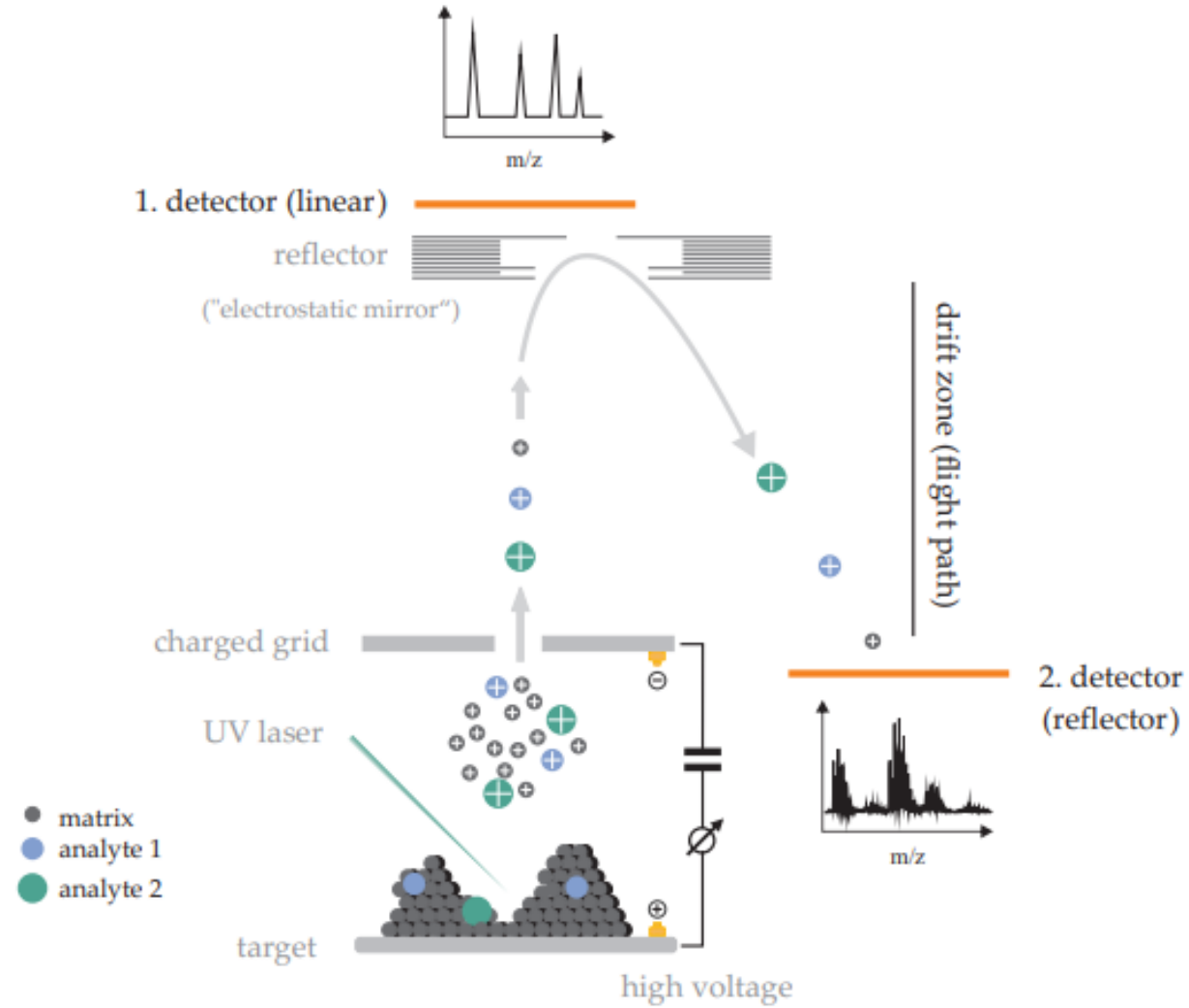

Figure 1. Simplified schema of the positive ionization matrix-assisted laser desorption/ionization-time-of-flight (MALDI-TOF) process occurring in the mass spectrometer (for details see text and Reference [18]). The influence of the detection using either the linear or the reflector mode is emphasized in the figure.

Leopold J et al. Biomolecules 2018;8:173.

Types of MALDI matrices

- classical organic matrices
  - most widely used:
  - proteins - α-cyano-4-hydroxycinnamic acid (CHCA), sinapinic acid (SA)
  - carbohydrates - 2,5-dihydroxybenzoic acid (DHB),
  - lipids – CHCA, DHB
- liquid crystalline matrices
- inorganic matrices
  - graphite

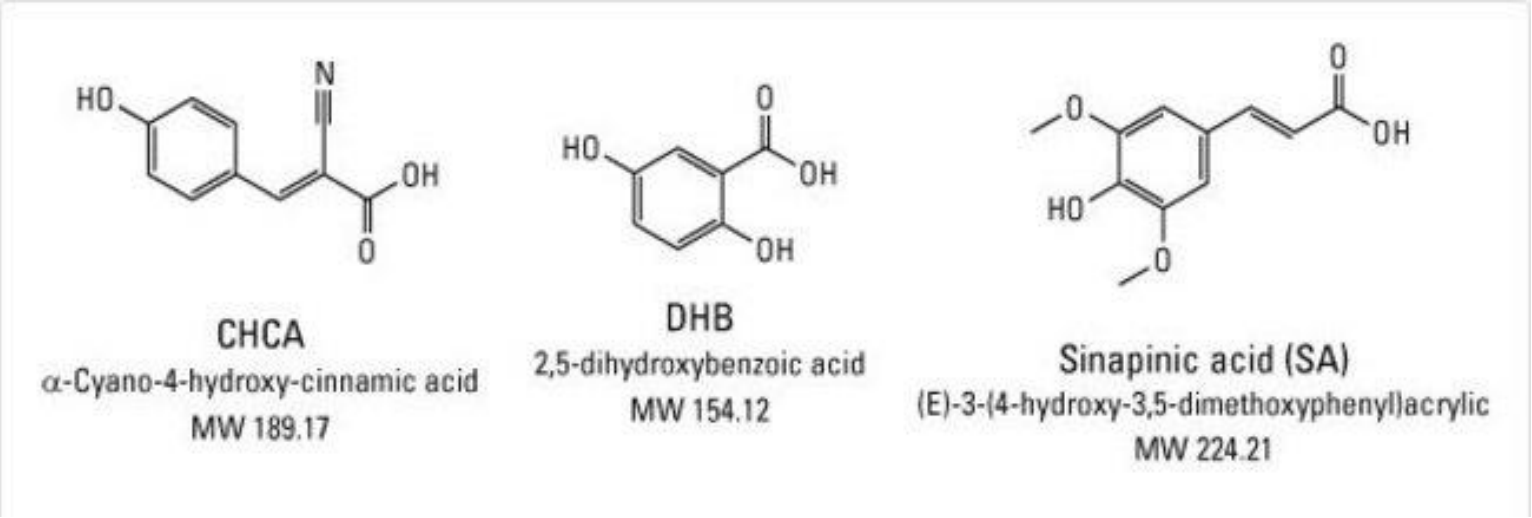

TABLE 2 List of common matrices used for UV-MALDI methods

Chromophore matrix(es)[a]	Sample type(s) analyzed
PA, HPA, 3-aminopicolinic acid	Oligonucleotides, DNA, and biopolymers
DHB	Oligosaccharides
CCA	Peptides and triacylglycerol
SA	Proteins
HABA	Peptides, proteins, glycoproteins
MBT	Peptides, proteins, synthetic polymers
DHAP	Glycopeptides, phosphopeptides
THAP	Oligonucleotides

[a] PA, picolinic acid; HPA, 3-hydroxypicolinic acid; SA, 3,5-dimethoxy-4-hydroxycinnamic acid; HABA, 2-(−4-hydroxyphenylazo)benzoic acid; MBT, 2-mercaptobenzothiazole; DHAP, 2,6-dihyroxyacetophenone; THAP, 2,4,6-trihydroxyacetophenone.

1. Quadrupole mass analyzers

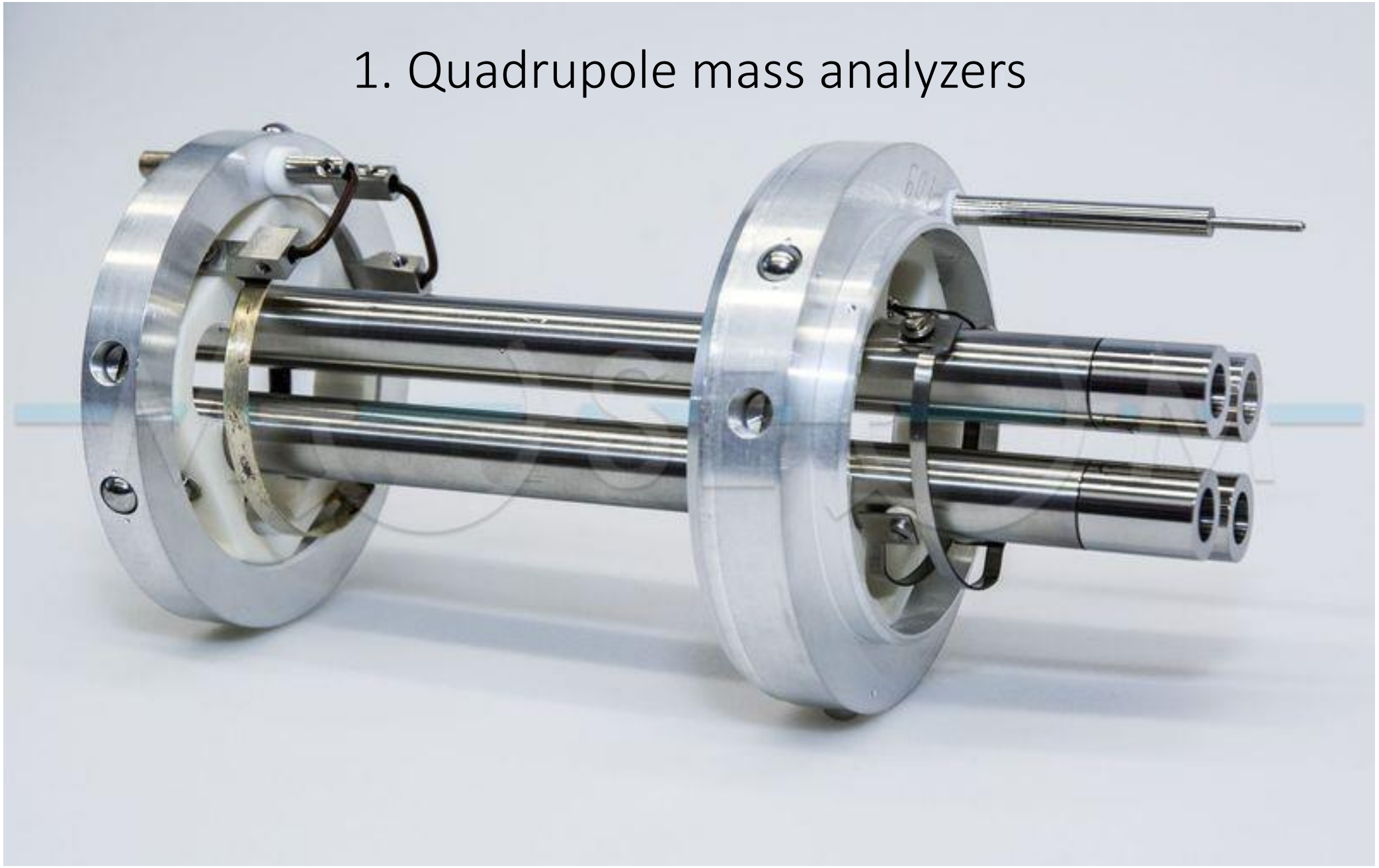

Operating principle

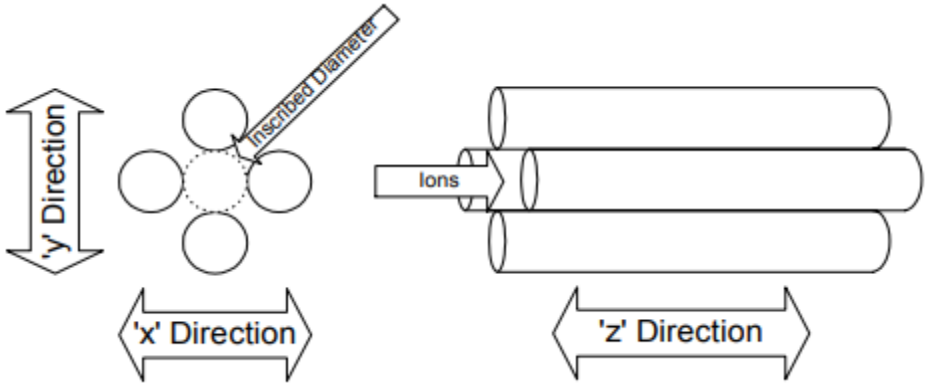

- Applied voltages:
  - fixed frequency oscillating RF voltage to generate harmonic ion trajectories
  - DC voltage difference between poles which defines mass resolution
  - DC offset voltage: defines axial ion energy

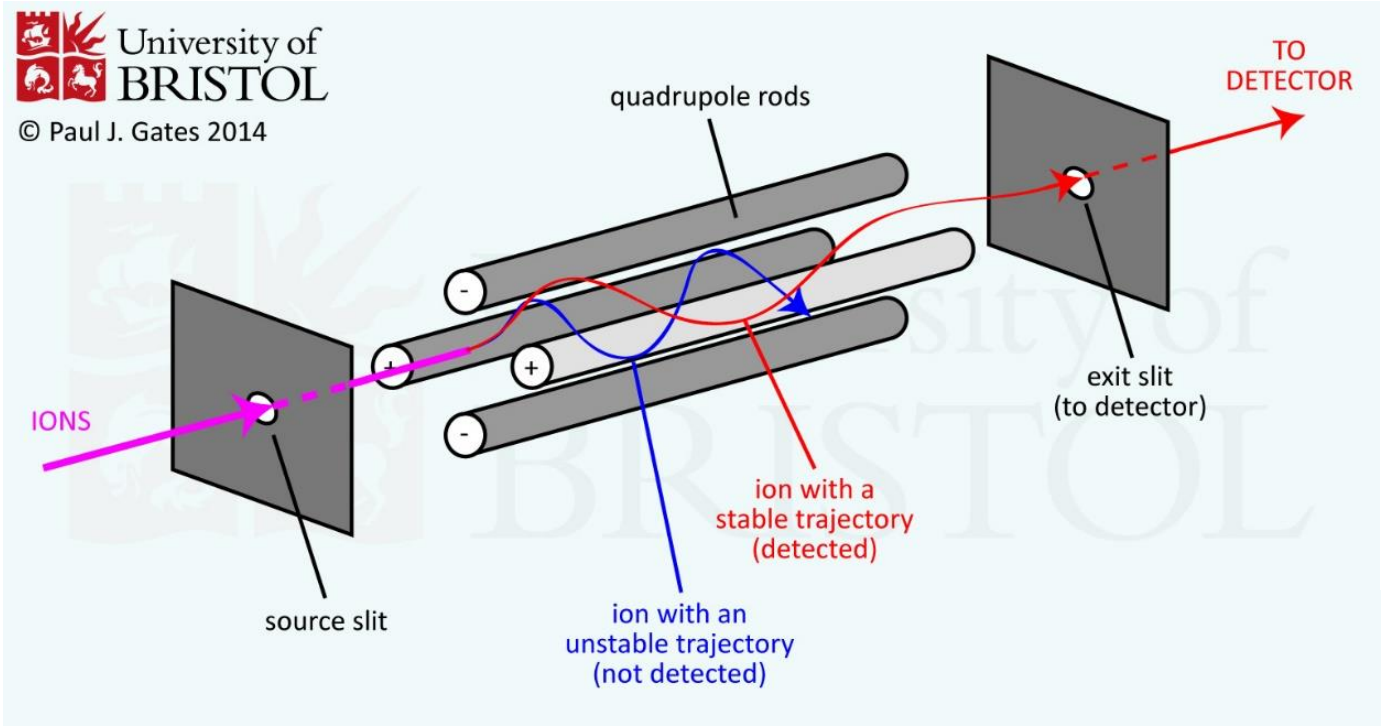

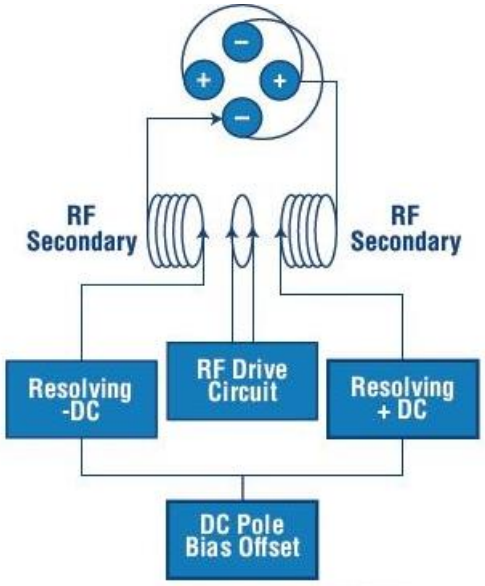

Types of tandem-in-space MS^2 experiments

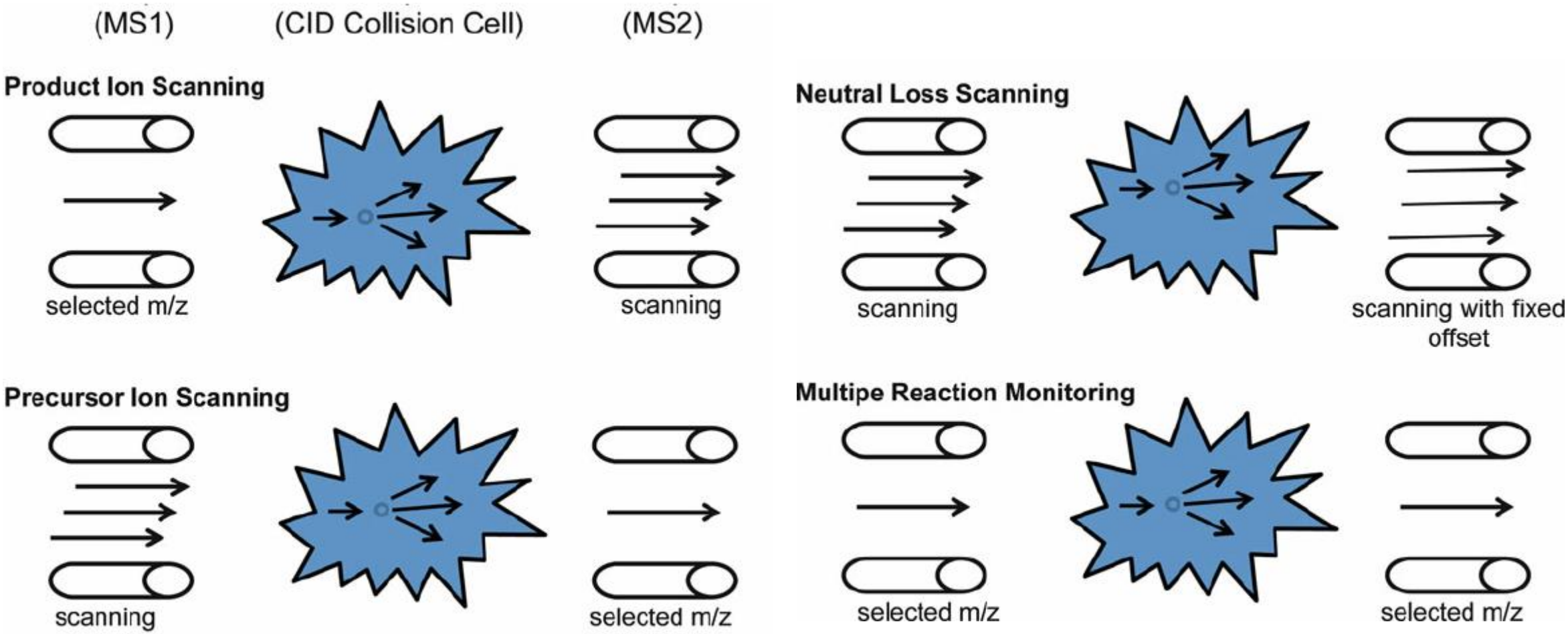

Screening neonates for inborn metabolic diseases

Samples are taken 48-72 h after birth

https://www.youtube.com/watch?v=vxshWngJ114

Targeted inborn disorders-I

- **Disorders of amino acid metabolism**
  - Phenylketonuria (Phenylalanine acculumates, 1:17 000)
  - Maple syrup disease (leucine, isoleucine and valine breakdown impaired, ketoacids accumulate, 1:150 000))
  - Tyrosinaemia types I and II (tyrosine accumulates, type I: 1:100 000)
  - Citrullinaemia I (urea cycle affected, ammonia accumulates, 1:57 000)
  - Arginosuccinate aciduria (urea cycle affected, ammonia accumulates, 1:70 000)
  - Homocystinuria (methionine breakdown impaired, homocysteine and methionine accumulate in plasma, 1:100 000)
- **Fatty acid oxidation disorders**
  - Short-chain acyl-CoA dehydrogenase deficiency (SCAD)
  - Middle-chain acyl-CoA dehydrogenase deficiency (MCAD)
  - Long-chain hydroxyacyl-CoA dehydrogenase deficiency (LCHAD)
  - Very long-chain acyl-CoA dehydrogenase deficiency (VLCAD)
  - Multiplex acyl-CoA dehydrogenase deficiency (MADD)
  - Carnitine-palmitoyl transferase deficiency (CPT-I, CPT-II)
  - Carnitine transport disorder (CT)

Targeted inborn disorders-II

- **Disorders of organic acid metabolism**
  - Beta-ketothiolase deficiency
  - Glutaric acidemia type 1
  - Isovaleric acidemia
  - Methylmalonic acidemia
  - Propionic acidemia
  - 3-hydroxy-3-methylglutaryl-CoA lyase deficiency
  - 3-methylcrotonyl-CoA carboxylase deficiency
  - Multiplex carboxylase deficiency

- **Endocrine and other disorders**
  - Hypothyreosis
  - Galactosemia
  - Biotinidase deficiency

The intracellular processing of fatty acids

Short-chain fatty acid: C2-C5

Middle-chain fatty acid: C6-C13

Long-chain fatty acid: C14-

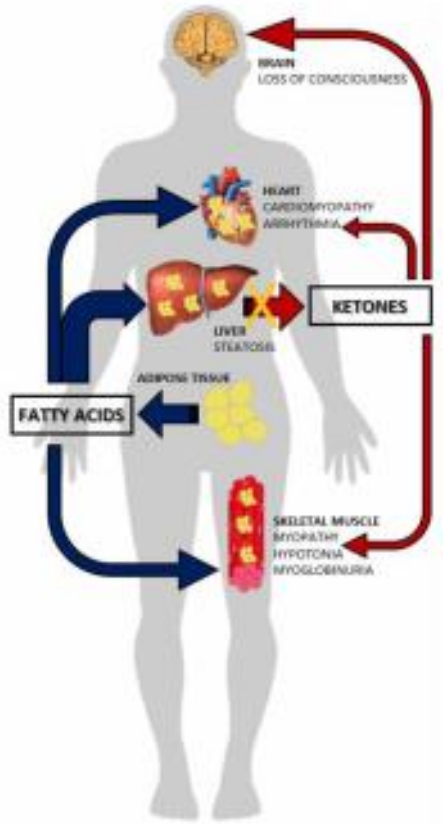

FIGURE 1. Fatty acids oxidation during fasting
During periods of fasting, fatty acids released from the adipose tissues are oxidized in the liver, skeletal muscle, and cardiac muscle for energy production. The brain does not directly utilize fatty acids, but oxidizes ketone bodies derived from β-oxidation of fatty acids in the liver. When fatty acid oxidation is defective, fats released from the adipose tissue cannot be oxidized, and accumulate in organs such as the skeletal and cardiac muscles, impairing their function. Moreover, the liver is unable to produce ketones bodies resulting in energy deficiency.

The intracellular processing of fatty acids

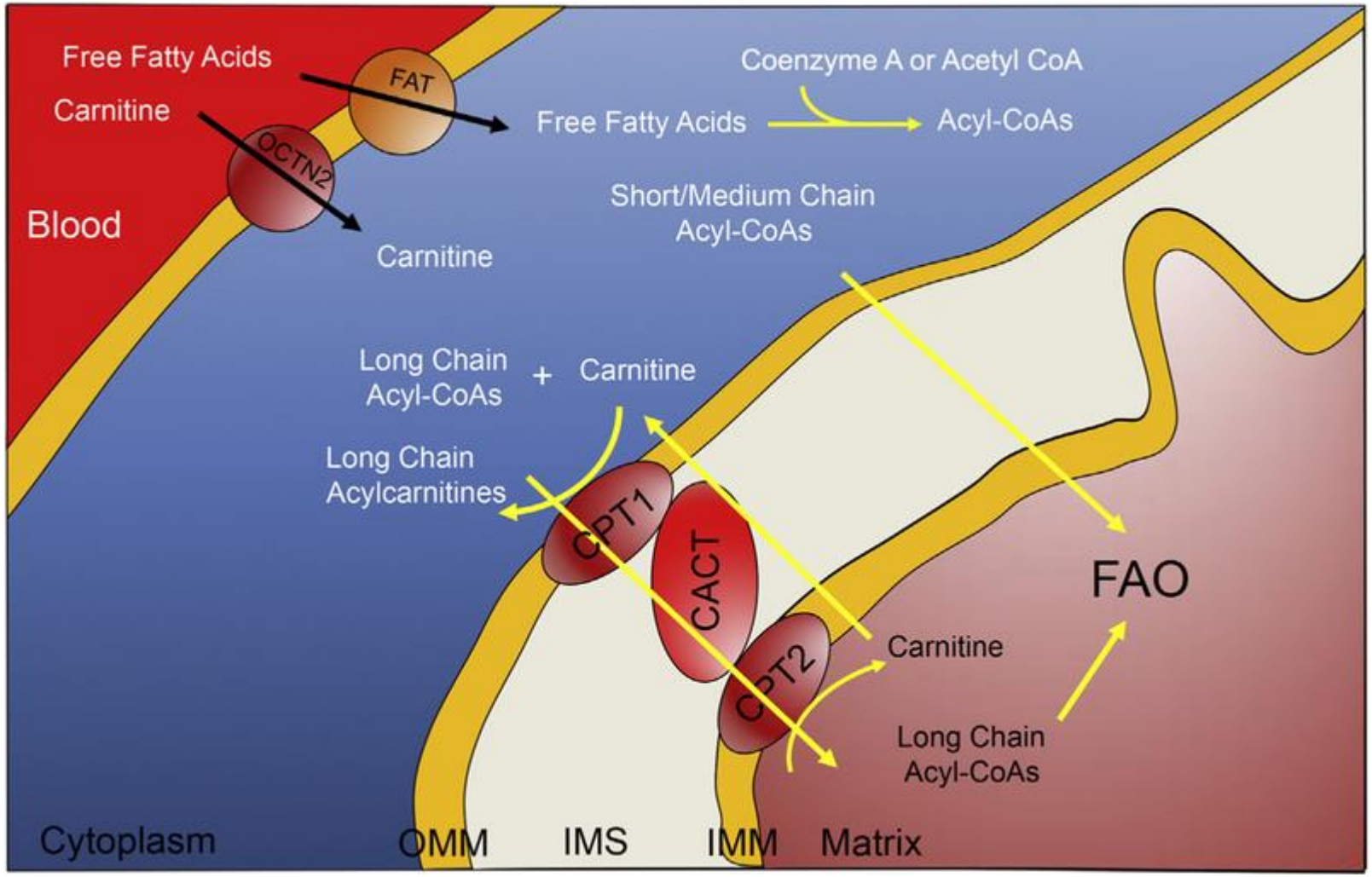

El-Gharbawy A et al. Pediatr Clin North Am 2018;65:317

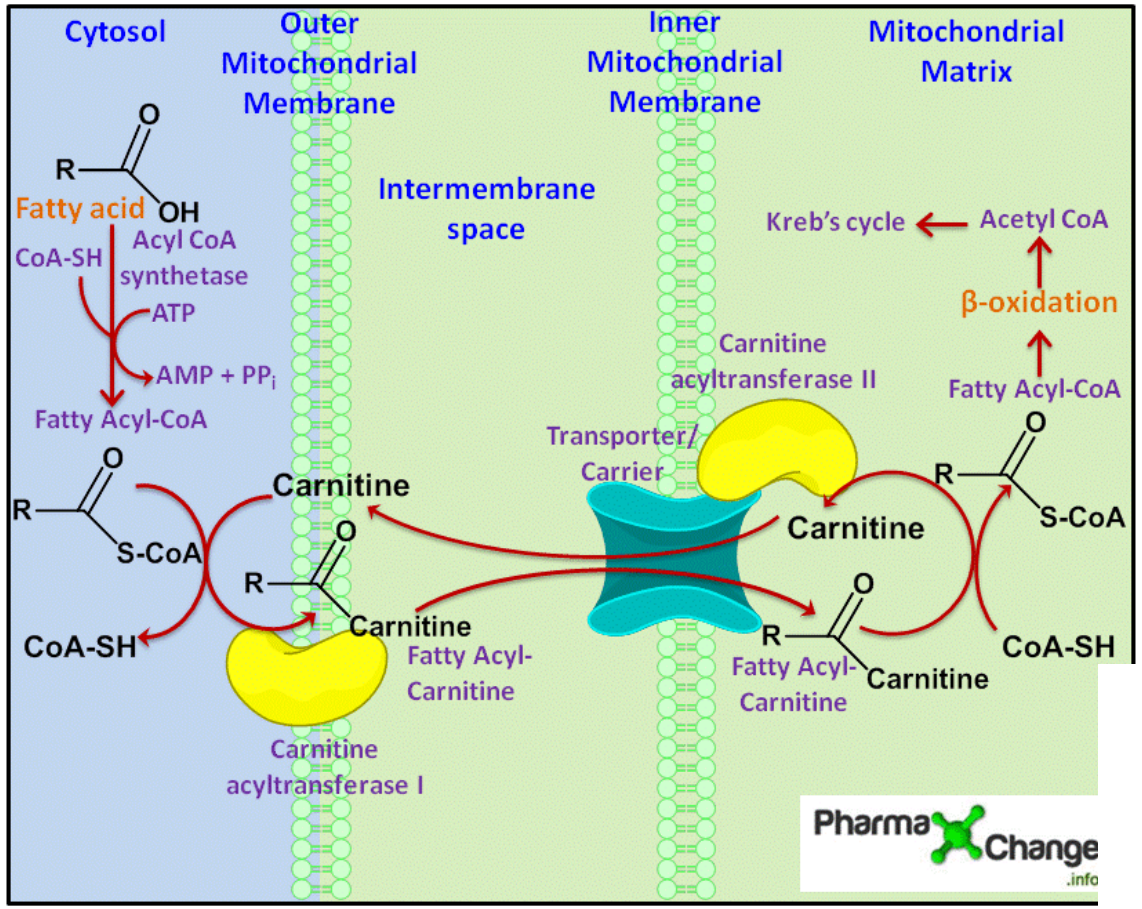
Cytosol
Outer Mitochondrial Membrane
Intermembrane space
Inner Mitochondrial Membrane
Mitochondrial Matrix
Fatty acid
Acyl CoA synthetase
CoA-SH
ATP
AMP + PPi
Fatty Acyl-CoA
Carnitine
Carnitine acyltransferase I
Fatty Acyl-Carnitine
Transporter/ Carrier
Carnitine acyltransferase II
Fatty Acyl-Carnitine
Carnitine
Kreb's cycle
Acetyl CoA
β-oxidation
Fatty Acyl-CoA
S-CoA
CoA-SH
PharmaXChange.info

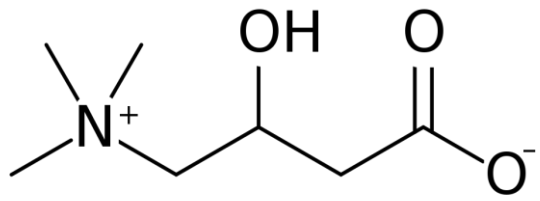

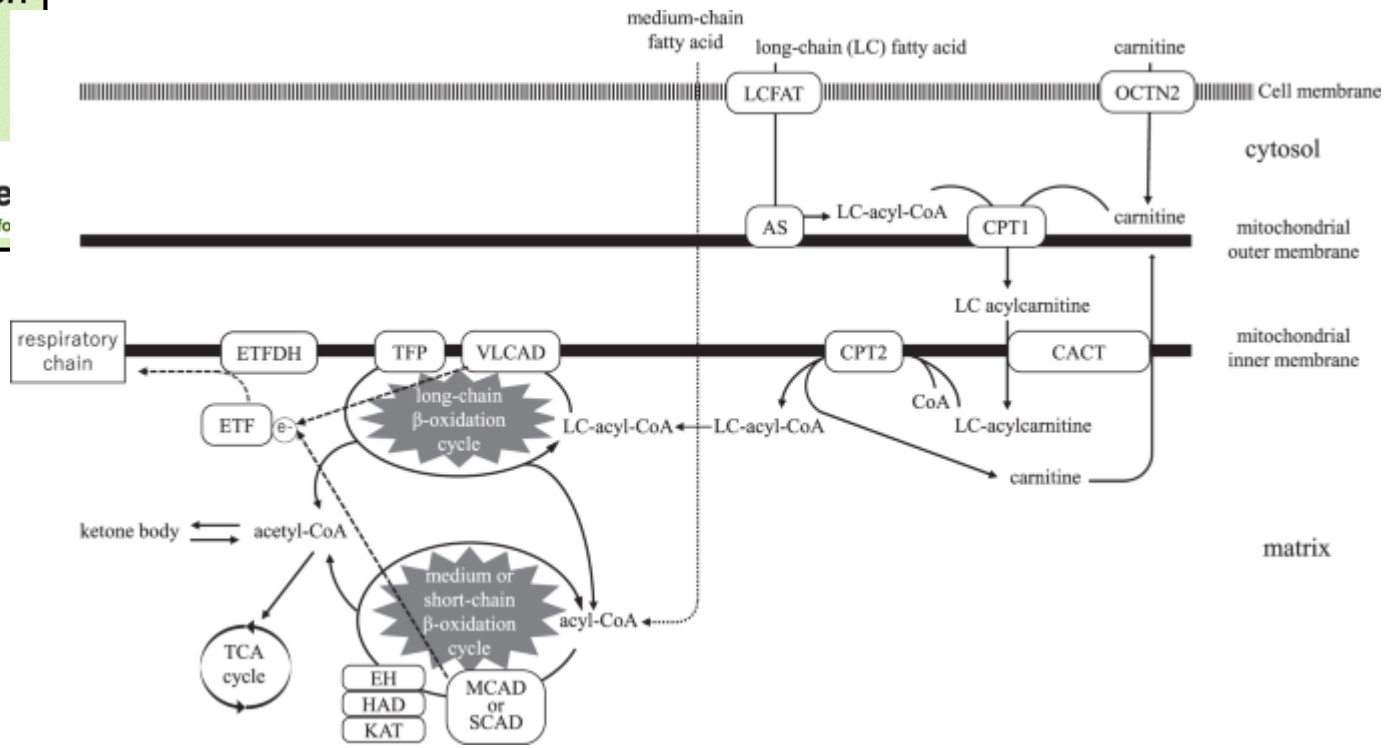
medium-chain fatty acid
long-chain (LC) fatty acid
carnitine
LCFAT
OCTN2
Cell membrane
cytosol
AS
LC-acyl-CoA
CPT1
carnitine
mitochondrial outer membrane
LC acylcarnitine
respiratory chain
ETFDH
TFP
VLCAD
CPT2
CACT
mitochondrial inner membrane
ETF
e-
long-chain β-oxidation cycle
LC-acyl-CoA
LC-acyl-CoA
CoA
LC-acylcarnitine
carnitine
ketone body
acetyl-CoA
matrix
medium or short-chain β-oxidation cycle
acyl-CoA
TCA cycle
EH
HAD
KAT
MCAD or SCAD

IEMs Associated with Myopathy	Inheritance	Clinical Phenotype
Defects in energy metabolism		
Carnitine shuttle defects		
Primary systemic carnitine deficiency	AR	HCM, hypotonia, muscle weakness, fatigue
Carnitine palmitoyl transferase deficiency type 2 (CPT2) deficiency[b]	AR	Muscle weakness, rhabdomyolysis, exercise intolerance (isolated muscle phenotype), CM, hepatomegaly, hypoglycemia, seizures, cystic kidneys (severe infantile)
Carnitine acylcarnitine translocase (CACT) deficiency	AR	CM, arrhythmias, muscle damage, hepatomegaly, hypoglycemia
FAODs		
VLCAD deficiency[b]	AR	HCM, arrhythmias, sudden death, muscle weakness, exercise intolerance, recurrent rhabdomyolysis, hypoketotic hypoglycemia, "Reye-like" hepatic syndrome
LCHAD deficiency[b]	AR	Sudden death, "Reye-like" hepatic syndrome, hypoketotic hypoglycemia, myopathy, recurrent rhabdomyolysis, CM, retinopathy
TFP deficiency[b]	AR	Sudden death, "Reye-like" hepatic syndrome, hypoketotic hypoglycemia, CM, recurrent, rhabdomyolysis, peripheral neuropathy
MAD deficiency	AR	Muscle weakness, CM, hypoglycemia, hepatopathy, respiratory dysfunction, encephalopathy, acidosis
Mitochondrial respiratory chain defects		
Respiratory chain complexes I-V	AR	Myopathy, CM, hepatopathy, Leigh syndrome, epilepsy, developmental delay ± lactic acidosis
Coenzyme Q deficiency		Myopathy, proteinuria, ataxia, low tissue Coenzyme Q, corrected by Coenzyme Q supplementation

El-Gharbawy A et al. Pediatr Clin North Am 2018;65:317

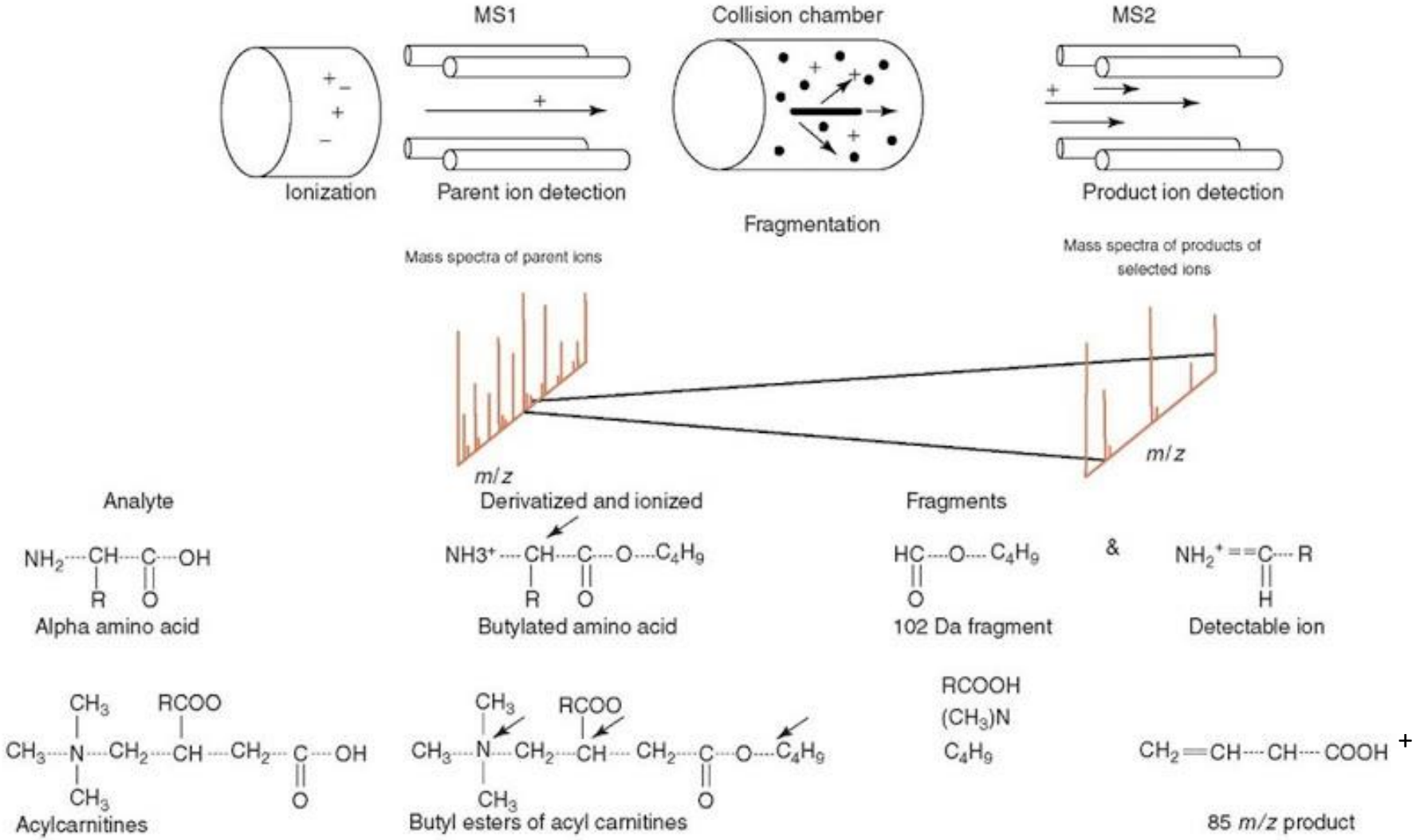

https://onlinelibrary.wiley.com/doi/epdf/10.1002/rcm.6856

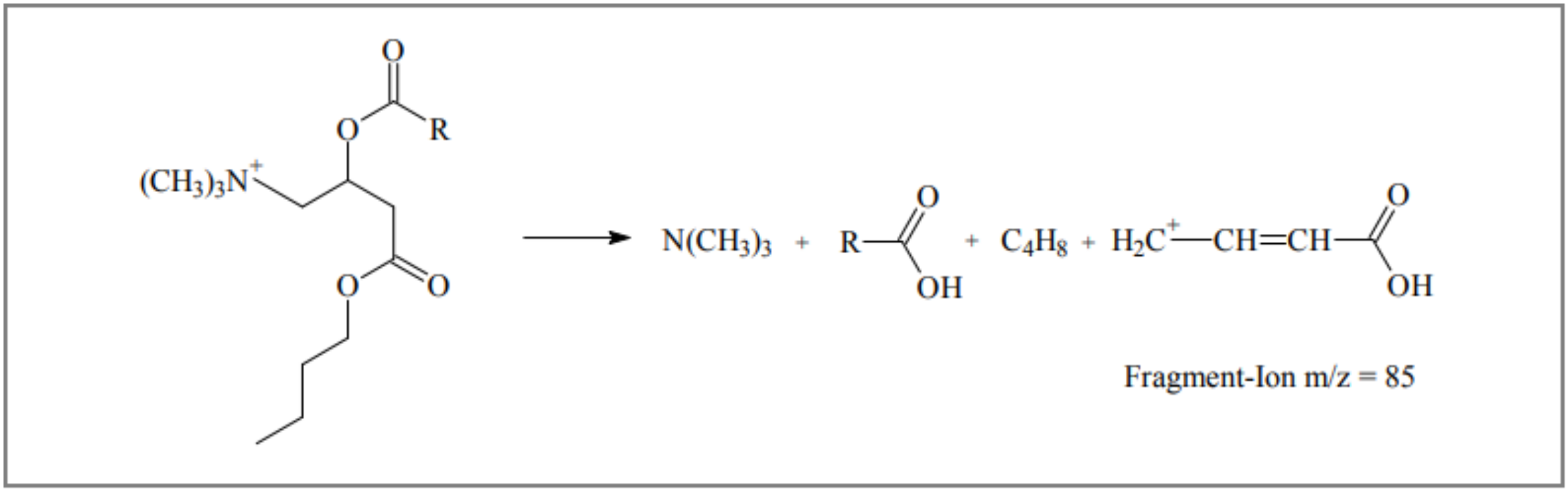

Abbildung 7: Fragmentierung der butylierten Acylcarnitine unter Abspaltung des charakteristischen Fragment-Ions m/z = 85
R = Alkylrest (z.B. R = CH_3 für Acetylcarnitin)

Assayed metabolites

- Amino acids with **neutral loss scan** m/z=102
  - Ala, Asp, Glu, Leu, Met, Phe, Tyr, Val

- Amino acids and succinylacetone (SUAC) using **multiple reaction monitoring**
  - Arg, Cit, Gly, Orn, Pro, SUAC

- Acylcarnitines and free carnitine using **precursor scan** of m/z=85
  - Carnitine, C2-carnitine, C3-carnitine, C4-carnitine, C5-carnitine, C6DC-carnitine, C6-carnitine, C8-carnitine, C10-carnitine, C12-carnitine, C14-carnitine, C16-carnitine, C17-carnitine

Sample preparation

- Punch out 3.2 mm dried blood spots into a 96-well plate
- add 200 µL internal standard mixture, agitate for 20 min
- transfer supernatant, evaporate to dryness
- add solution of derivatizing reagent, incubate
- evaporate to dryness
- add reconstitution solution, agitate briefly
- inject aliquot into the LC-MS/MS system

Analysis using LC-MS/MS

- HPLC: isocratic, flow-injection analysis is used (no analytical column)
- ionization: (+) ESI
- mass analyzer: triple quadrupole

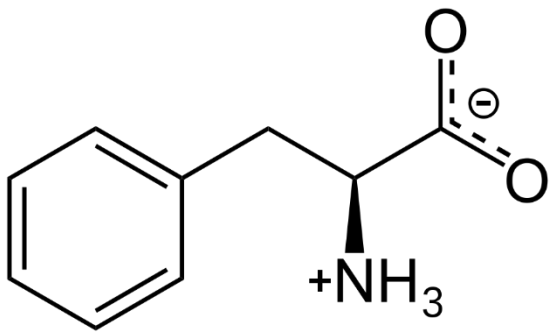

$C_9H_{11}NO_2$
165.2

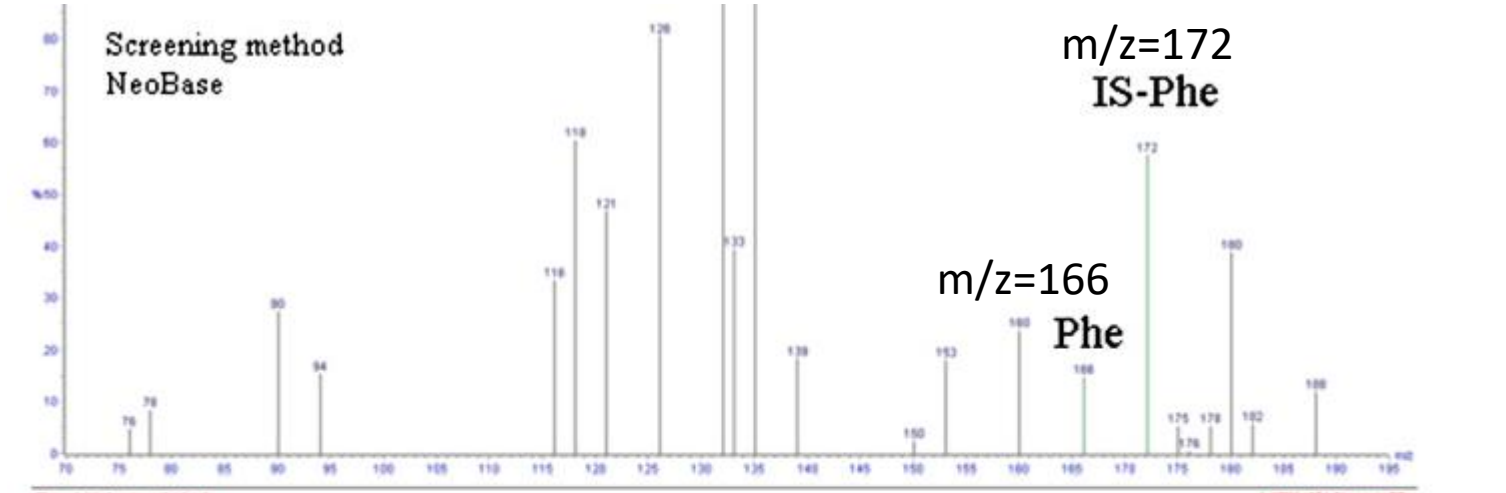

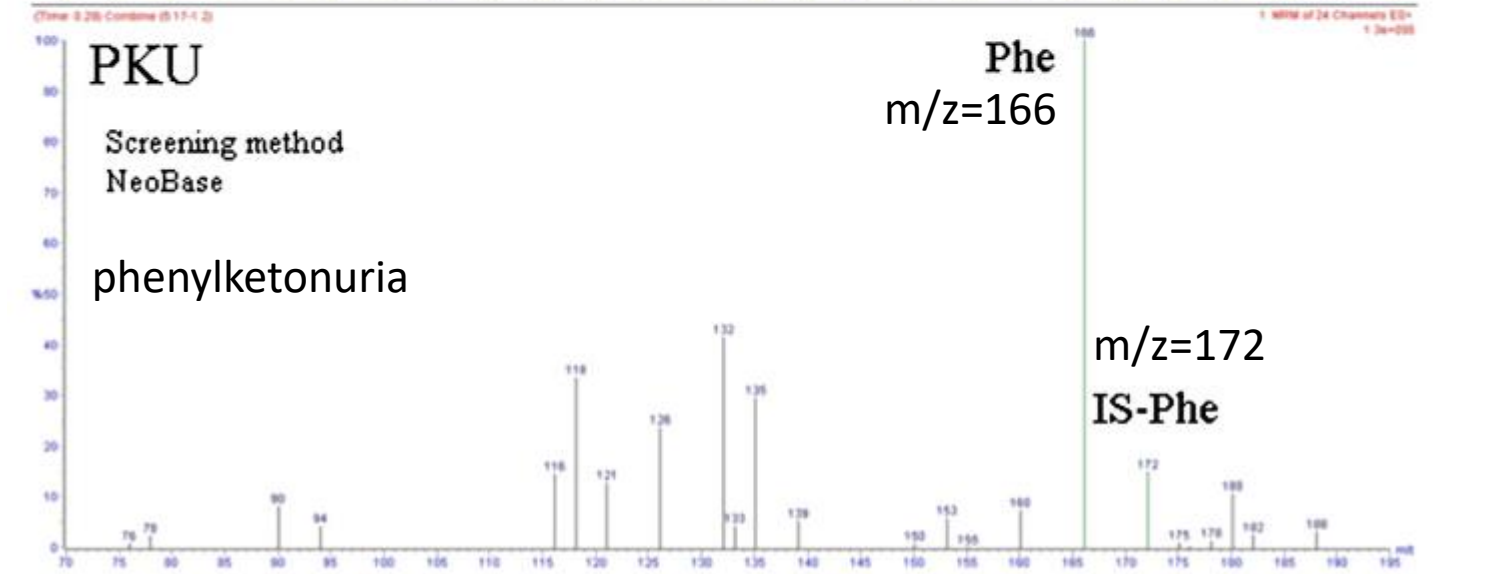

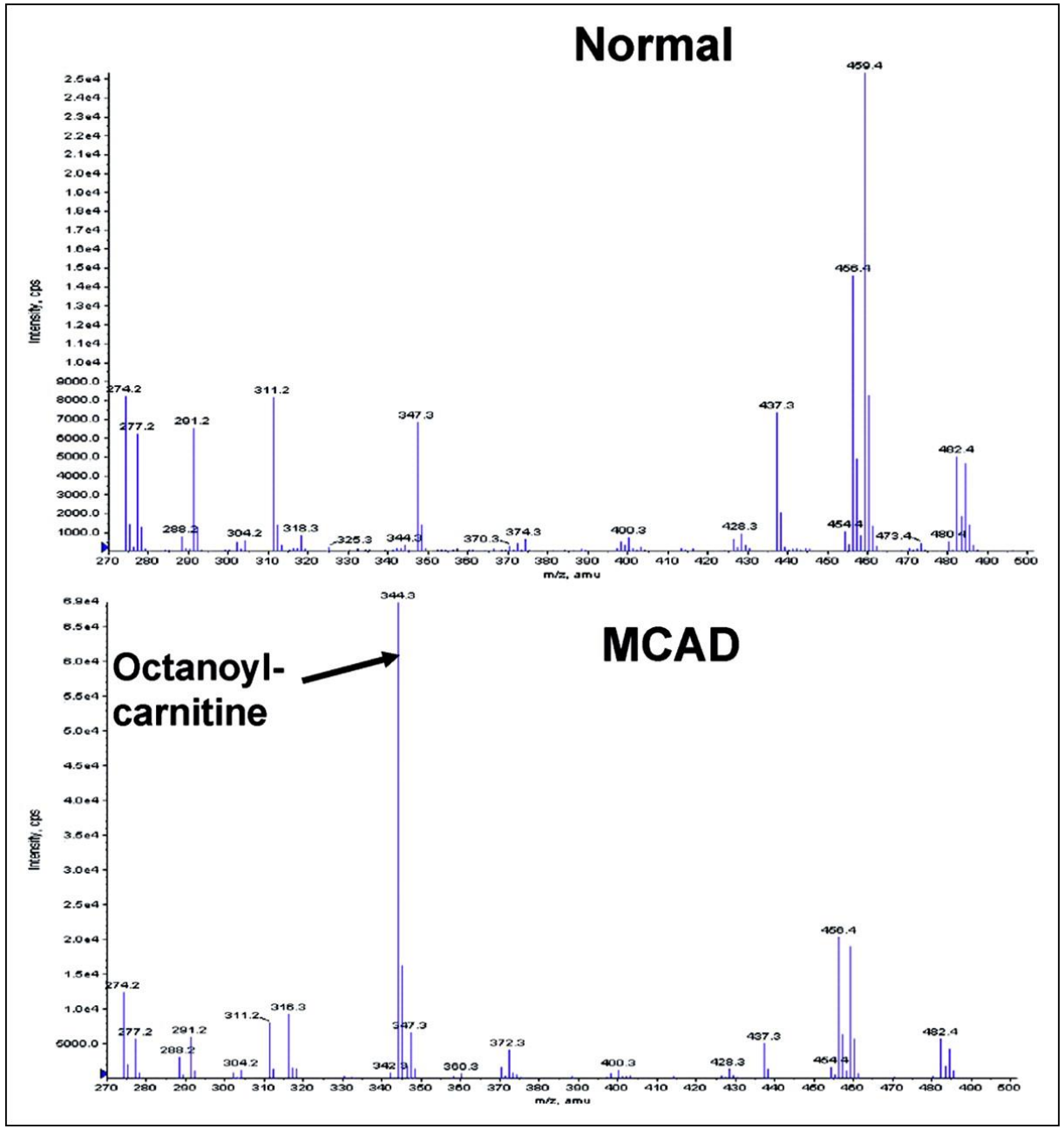

Cowan T NeoREviews 2005;6:e539.

Diagnostic applications of the analysis of serum steroid profiles using LC-MS/MS

- Screening, diagnosis and therapy monitoring:
  - Congenital adrenal hyperplasia
    - 21-hydroxylase deficiency (CYP21A2)
    - 11β-hydroxylase deficiency
    - 17α-hydroxylase/17-20 lyase deficiency (CYP17A)
    - 3β-hydroxysteroid dehydrogenase deficiency
    - Congenital lipoid adrenal hyperplasia
    - P450 oxydoreductase deficiency
  - Cushing syndrome
  - Primary/secondary adrenocortical insufficiency
  - hyperaldosteronism
  - adrenocortical tumors
  - other functional changes in the HPA axis
  - adverse effects of drug therapies
  - Polycystic ovary syndrome

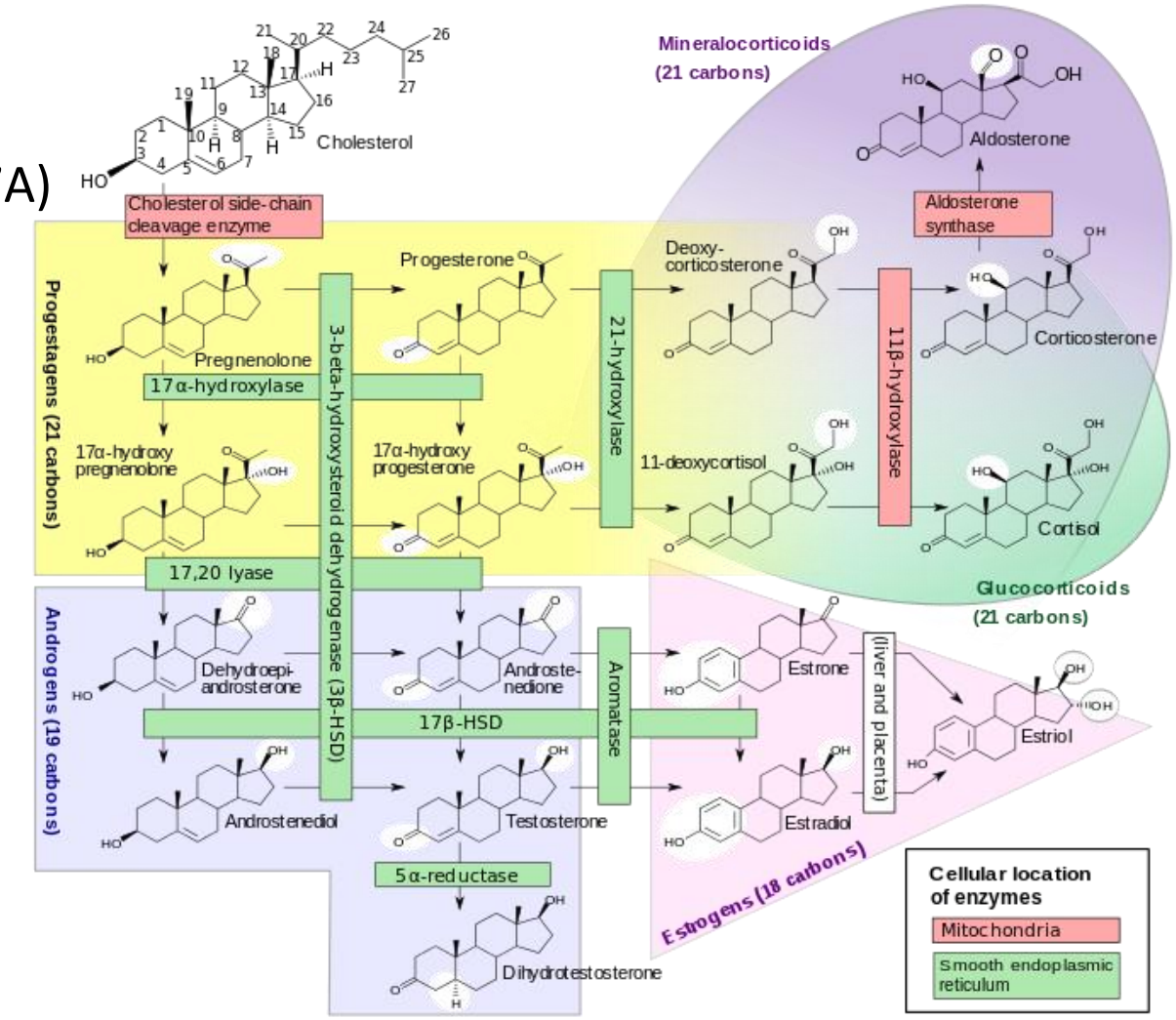

Figure 3. **The cortisol–cortisone shuttle.**

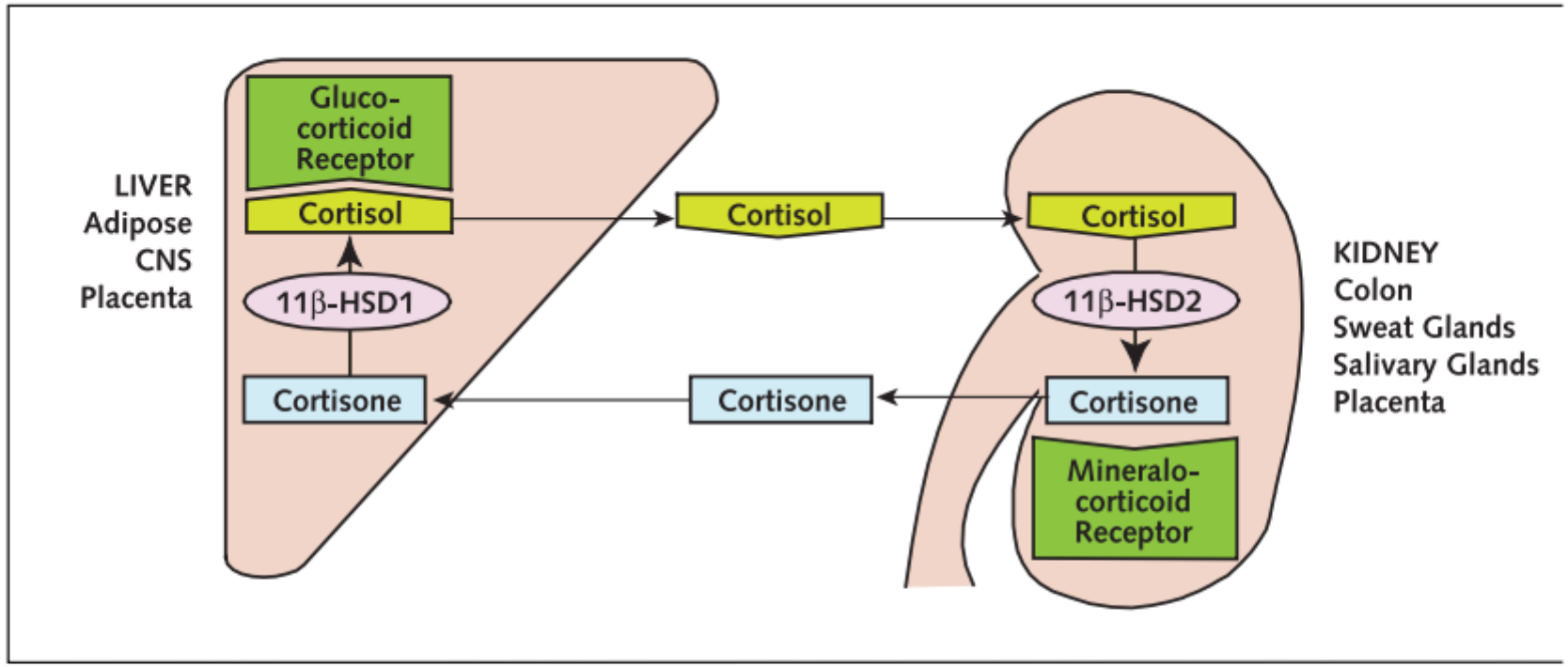

The effect of cortisol on the mineralocorticoid receptor (for example, in the kidney) is prevented by metabolism to inactive cortisone by the enzyme 11β-hydroxysteroid dehydrogenase type 2 (*11β-HSD2*). Cortisone can be reactivated to cortisol by the enzyme 11β-hydroxysteroid dehydrogenase type 1 (*11β-HSD1*). When cortisol level is very high (as in the Cushing syndrome), not all of the excess cortisol can be inactivated to cortisone, and the effects of mineralocorticoid excess (for example, hypertension and hypokalemia) can occur. Modified from Seckl JR, Walker BR. Minireview: 11β-hydroxysteroid dehydrogenase type 1—a tissue-specific amplifier of glucocorticoid action. Endocrinology. 2001;142(4):1371-6, with permission from The Endocrine Society (19). CNS = central nervous system.

Laboratory parameters

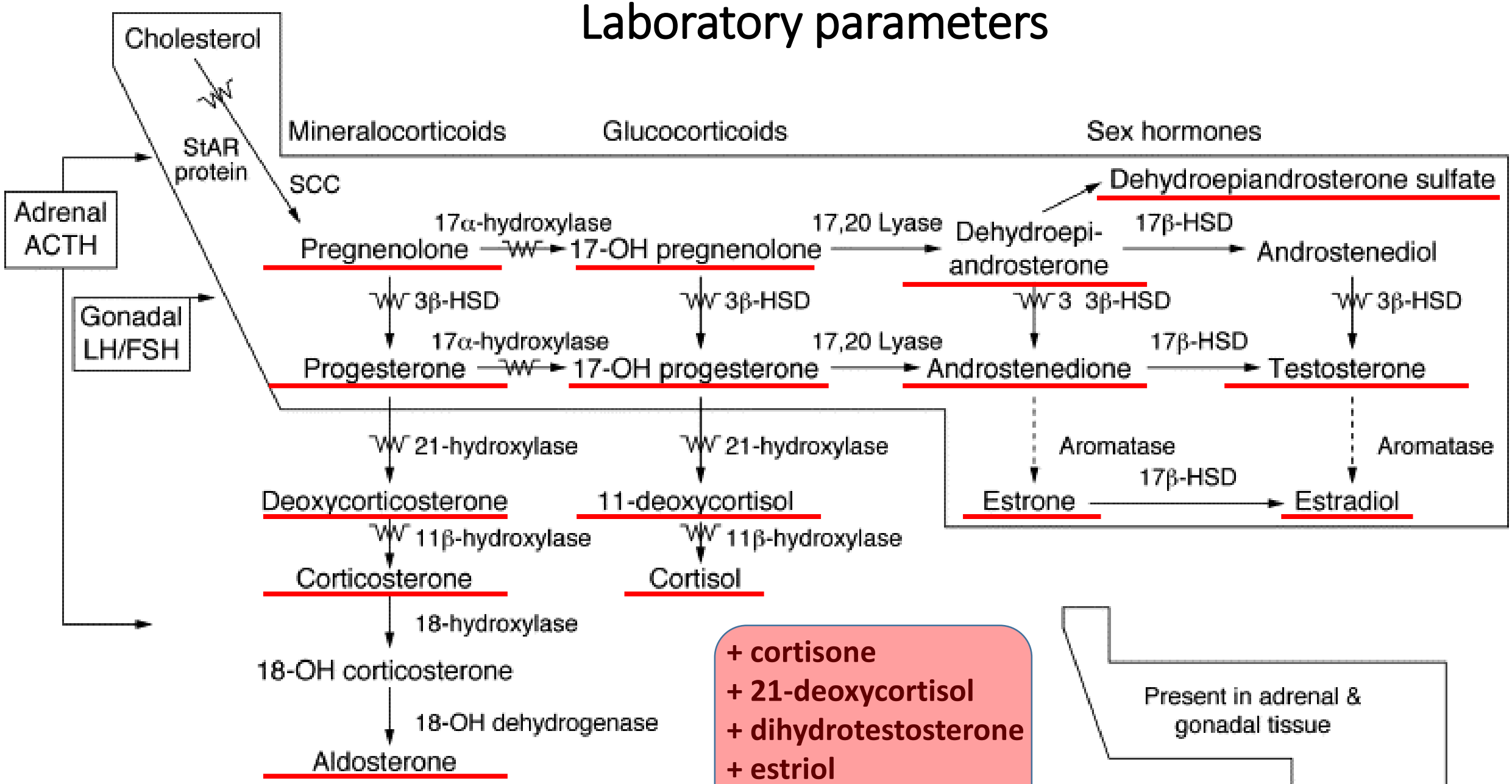

Pang S. Trends Endocrinol Metab 1998;9:82-6.

Method in serum:

- sample preparation:
  - 200 µL serum + 600 µL methanol containing internal standards
  - vortex
  - Dilute 400 µL with 400 µl water
  - Apply to Strata-X solid phase extraction cartridge
  - Wash with water-methanol 3:1
  - Elute with acetonitrile-methanol 1:1
  - Evaporate to dryness
  - Reconstitute with 50 µL water-methanol 1:1

- analysis: LC-ESI(+)-MS/MS, run time: 2x6 min
  - SP: C18 50x2.1 mm, 1.7 µm + biphenyl 50x2.1 mm, 1.7 µm
  - MP: water (A), methanol (B), both containing 0.1% formic acid
  - sample volume: 5 µL, 15 °C
  - FR: 0.33 mL/min
  - CTO: 35 °C
  - MS mode: MRM

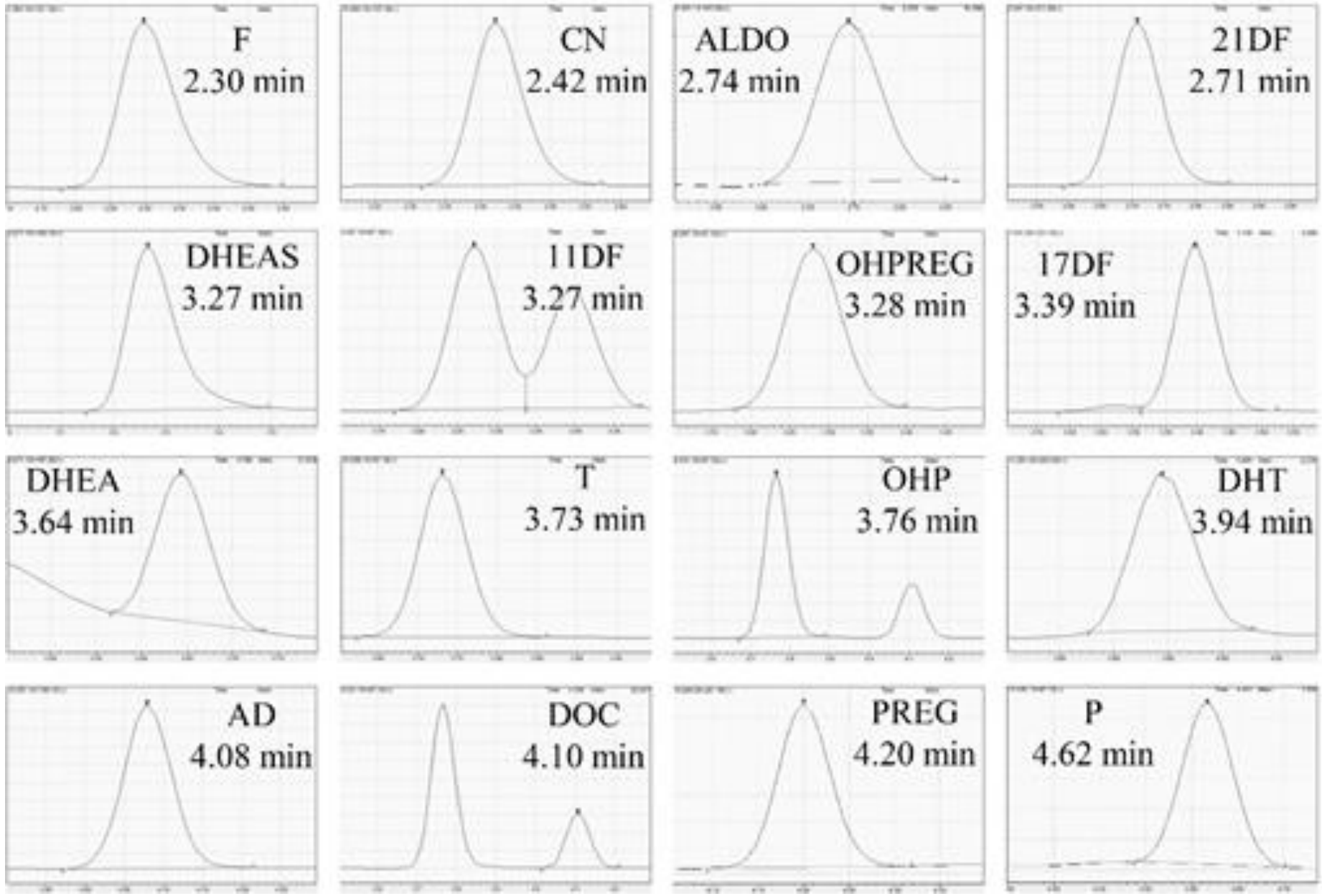
F
2.30 min
CN
2.42 min
ALDO
2.74 min
21DF
2.71 min
DHEAS
3.27 min
11DF
3.27 min
OHPREG
3.28 min
17DF
3.39 min
DHEA
3.64 min
T
3.73 min
OHP
3.76 min
DHT
3.94 min
AD
4.08 min
DOC
4.10 min
PREG
4.20 min
P
4.62 min

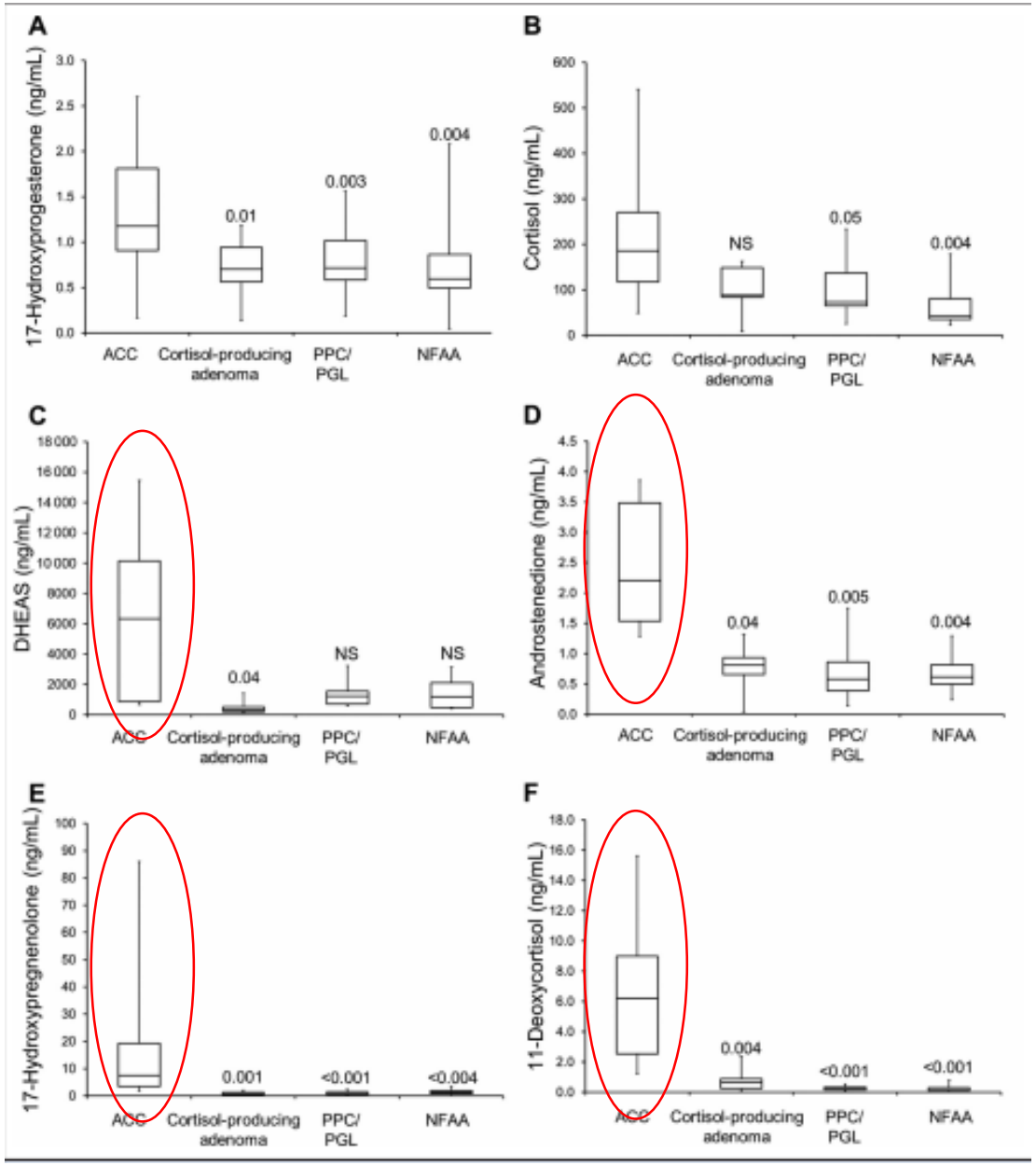

Taylor DR et al. Clin Chem 2017;63:1836.

Healthy adrenal cortex (boy, 6 y)

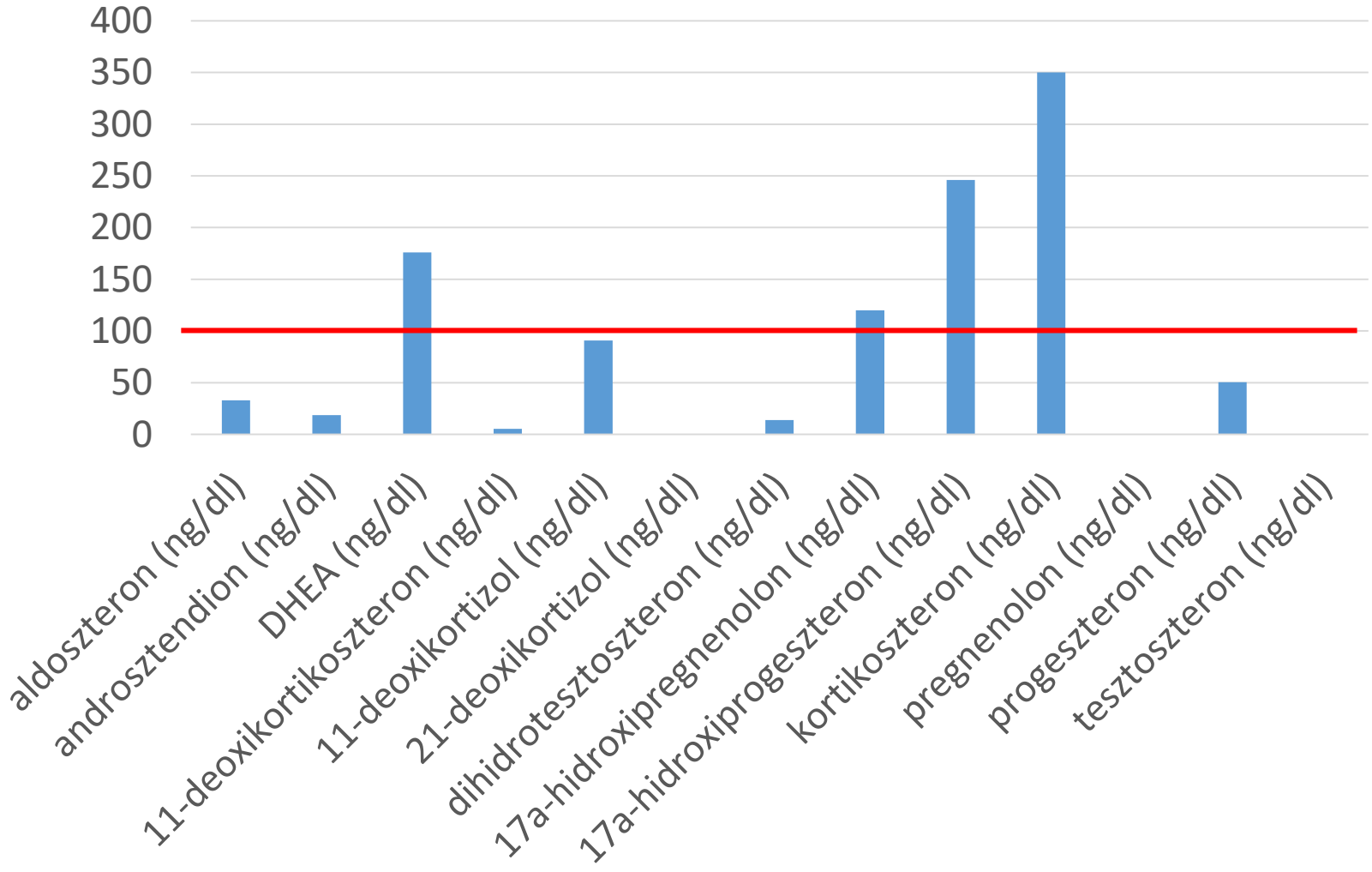

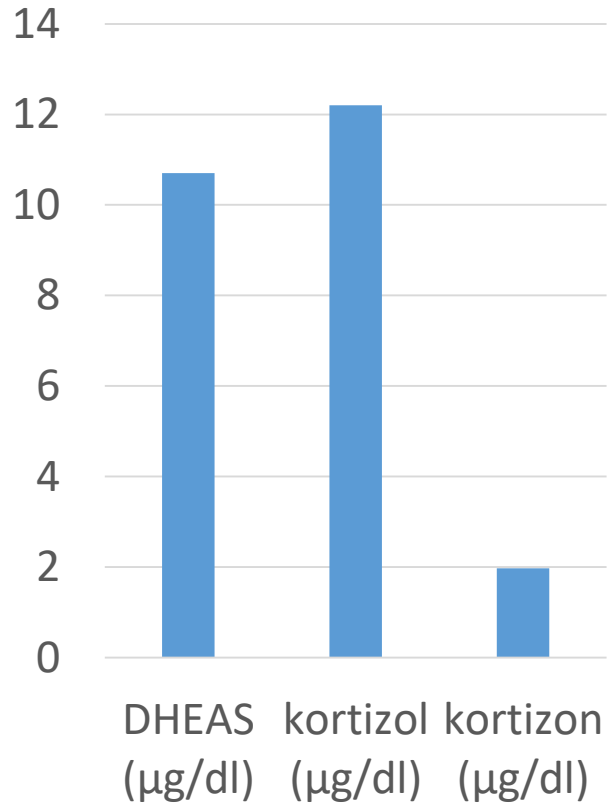

Results of ACTH stimulation test in healthy girl (11y)

Analyte	Concentration before ACTH stimulation	Concentration after ACTH stimulation
aldosterone (ng/dL)	<2.0	7.9
androstenedione (ng/dL)	120	120
DHEA (ng/dL)	315	483
DHEAS (µg/dL)	<10	14
11-deoxycorticosterone (ng/dL)	6.4	24.7
11-deoxycortisol (ng/dL)	33.9	151
21-deoxycortisol (ng/dL)	9.7	48.2
dihydrotestosterone (ng/dL)	10.9	13.1
17α-hydroxypregnenolone (ng/dL)	<30	103
17α-hydroxyprogesterone (ng/dL)	191	484
corticosterone (ng/dL)	100	1687
cortisol (µg/dL)	18.4	23.6
cortisone (µg/dL)	2.8	2.7
pregnenolone (ng/dL)	<30	<30
progesterone (ng/dL)	56.7	127
testosterone (ng/dL)	45.4	33.0

Results of a dexamethasone suppression test (girl, 16y)

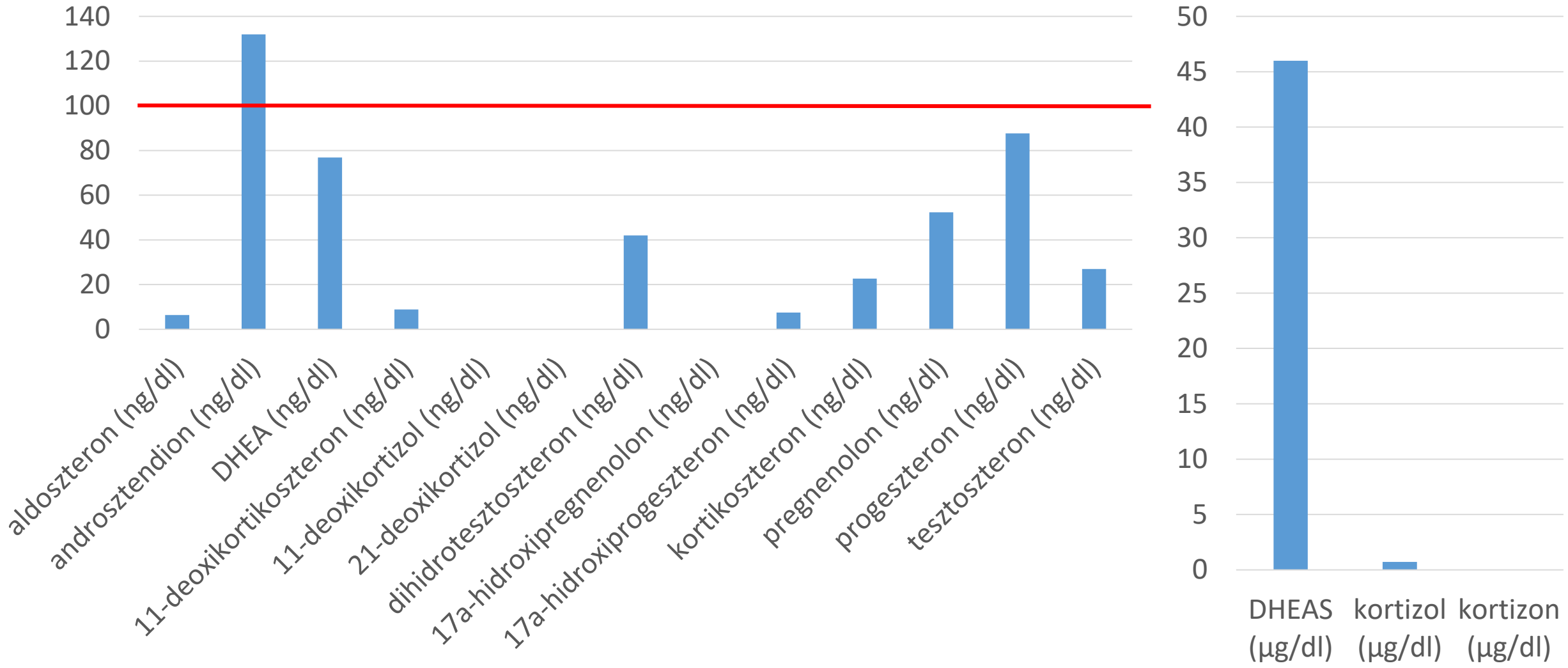

Classical congenital adrenal hyperplasia (boy, 11y)

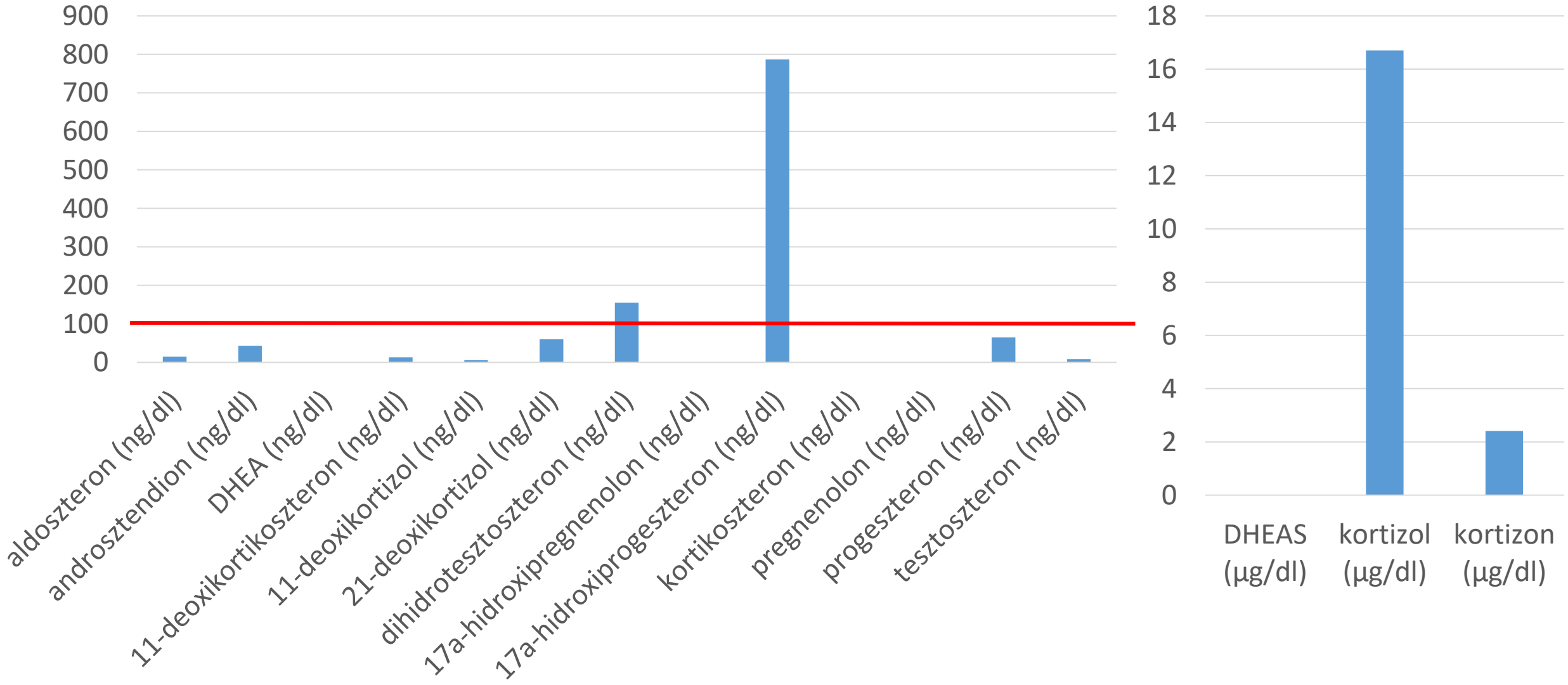

Time-of-flight mass analyzers

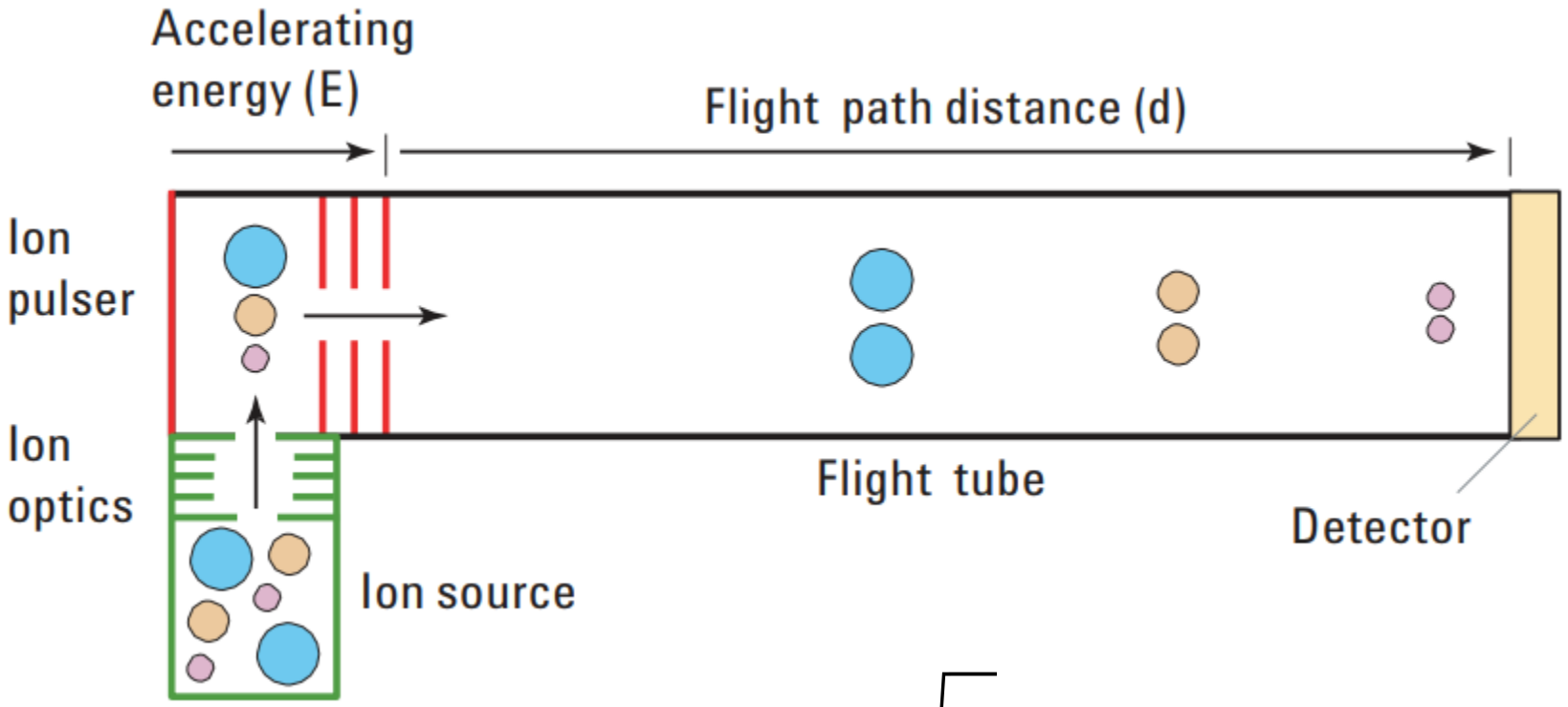

$$t \sim \sqrt{\frac{m}{q}}$$

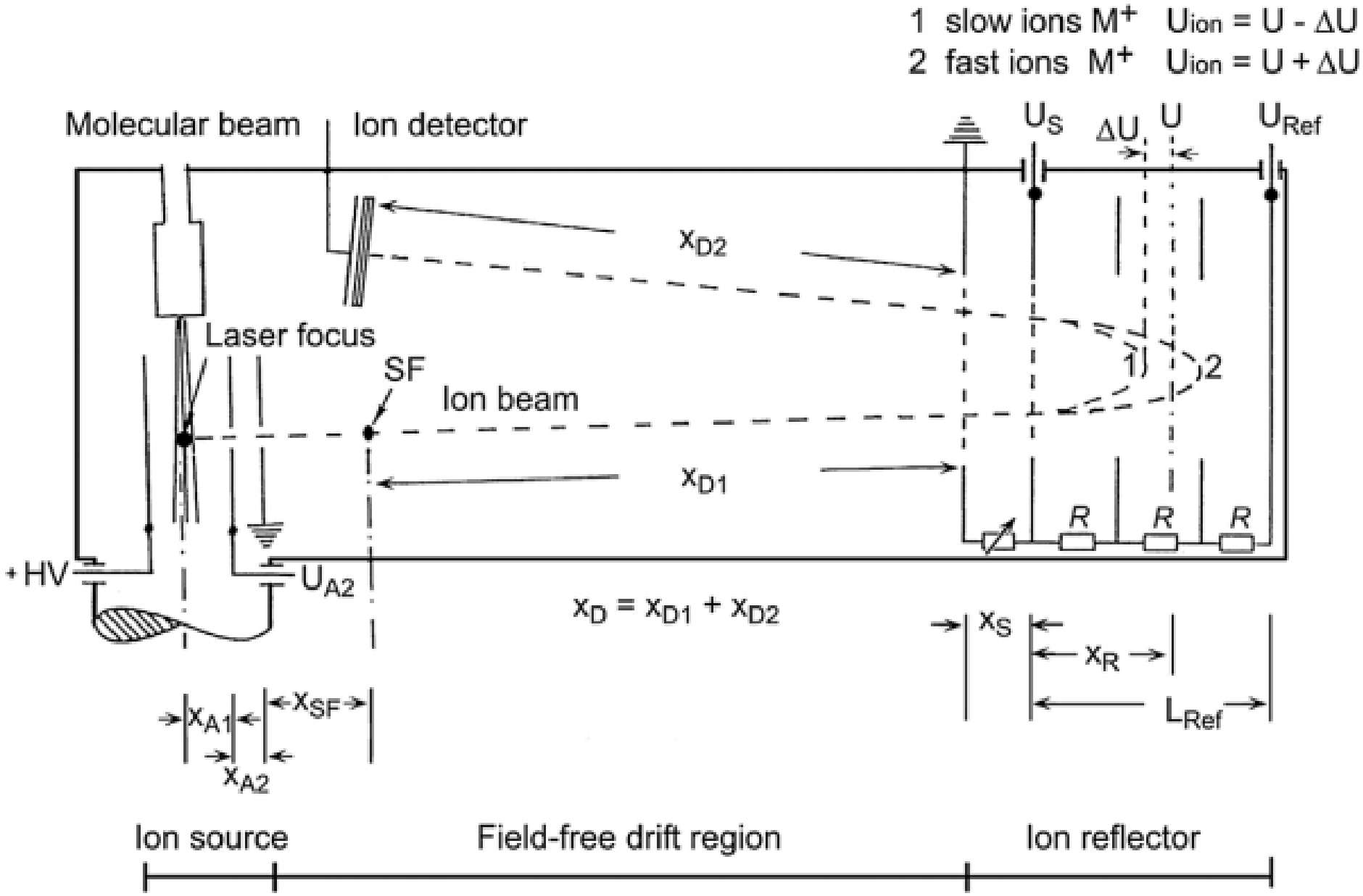

Boesl U. Mass Spectrom Rev 2017; 36:86.

Quadrupole-time-of-flight mass analyzers

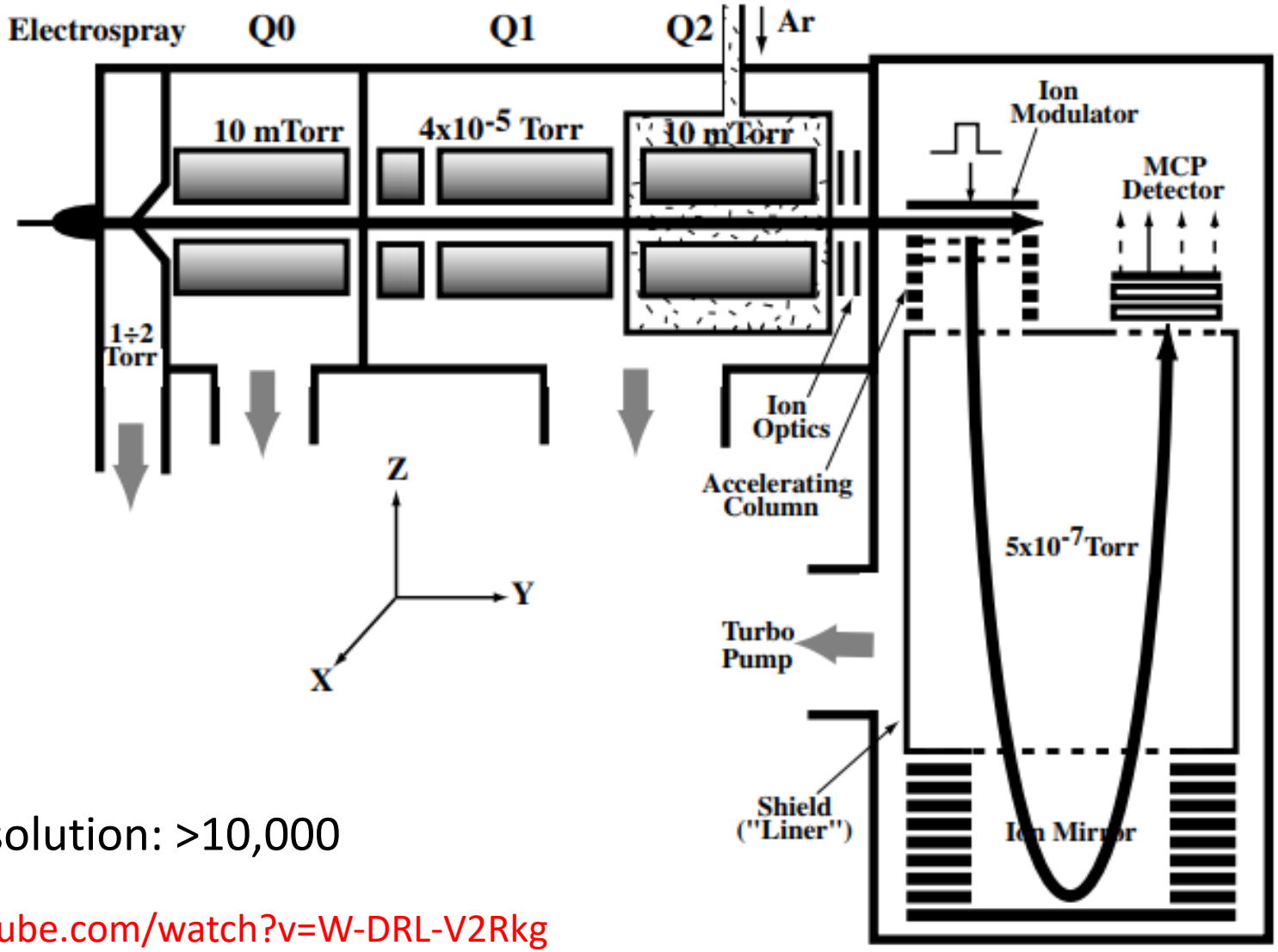

Resolution: >10,000

https://www.youtube.com/watch?v=W-DRL-V2Rkg

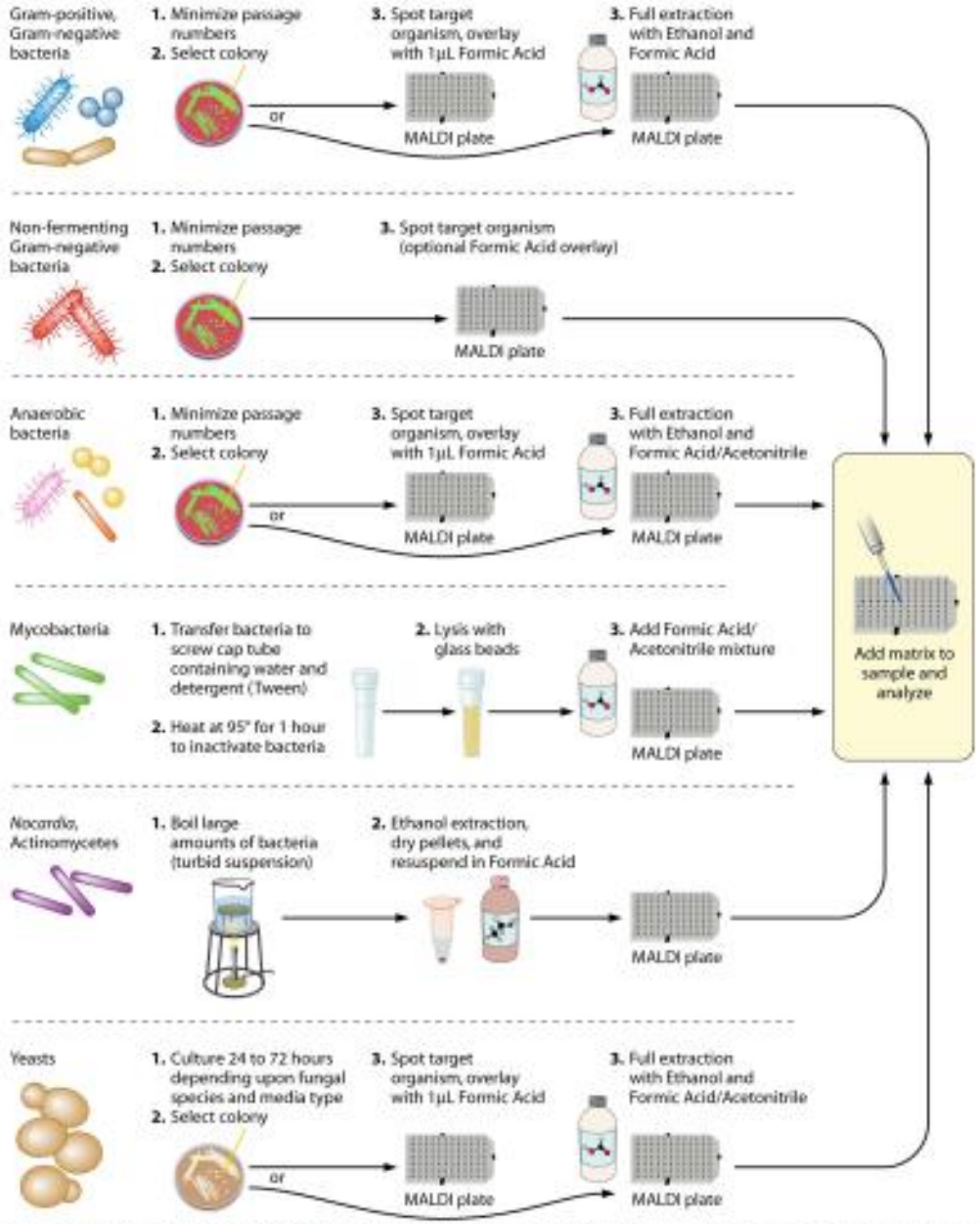

FIG 3 Additional suggestions for MALDI-TOF MS sample preparations for use with different classes of microbes. Different groups of microorganisms vary fundamentally in their cellular composition and architecture. These differences have been demonstrated to affect the quality of spectra generated during MS experiments and, thus, the accuracy of MALDI-TOF MS-derived identifications. As such, investigators from a number of independent studies have evaluated different methods for sample preparation of different groups of microorganisms, ranging directly from intact-cell to full-protein-extraction-based methodologies. Results from these studies are summarized here. Proper biological safety precautions should be followed with respect to dangerous members of these groups of organisms.

Clarke AE et al. Clin Microbiol Rev 2013;26:547-603.

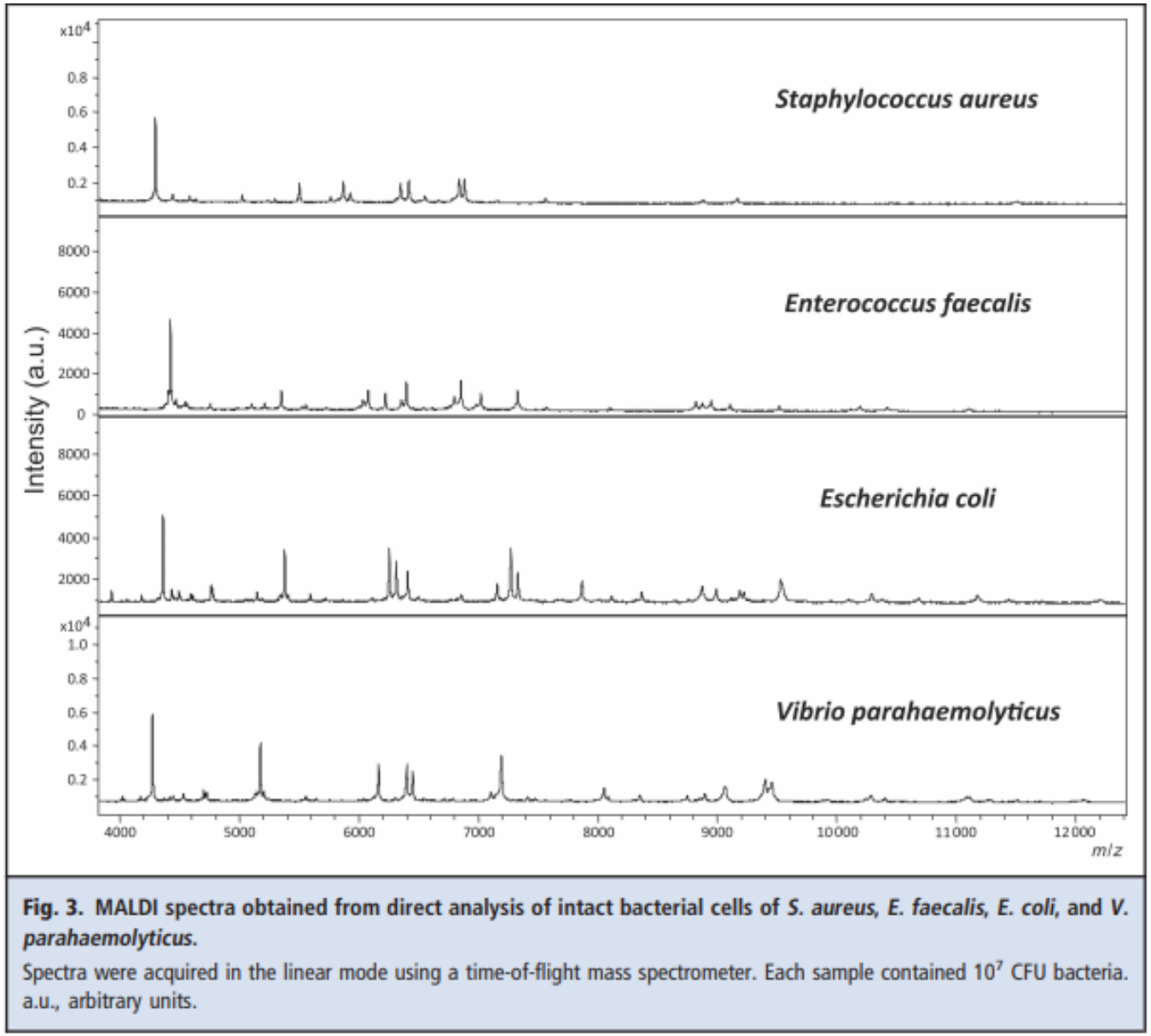

Fig. 3. MALDI spectra obtained from direct analysis of intact bacterial cells of *S. aureus*, *E. faecalis*, *E. coli*, and *V. parahaemolyticus*.

Spectra were acquired in the linear mode using a time-of-flight mass spectrometer. Each sample contained 10^7 CFU bacteria. a.u., arbitrary units.

Ho YP, Reddy PM. Clin Chem 2010;56:525.

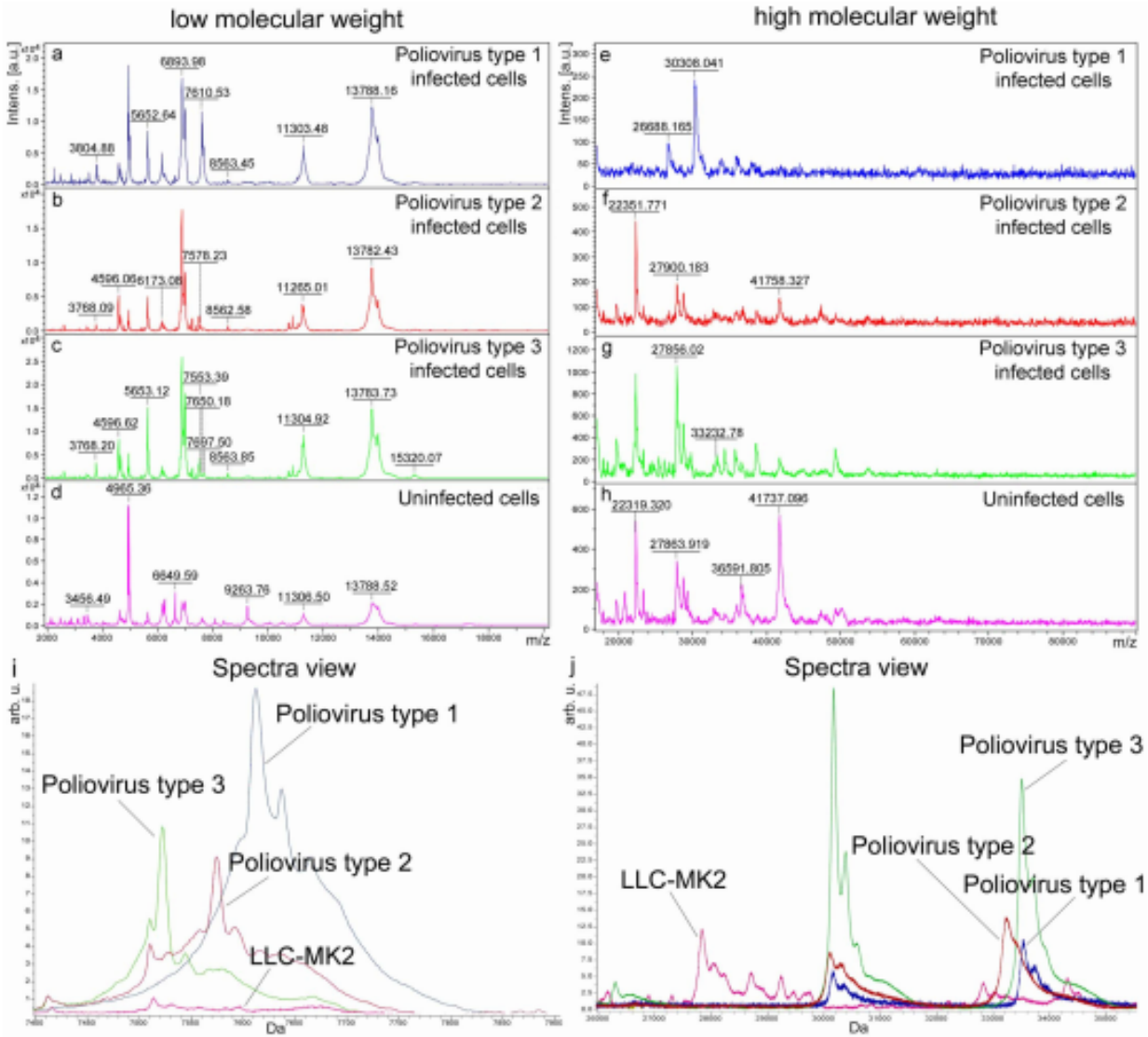

Figure 2 | Representative MALDI-TOF mass spectra of Sabin poliovirus-infected and uninfected LLC-MK2 cells and comparative analysis by ClinPro Tools software. The spectra of LLC-MK2 cells infected with human poliovirus types 1, 2, 3 ("Poliovirus type 1-infected cells", "Poliovirus type 2-infected cells", "Poliovirus type 3-infected cells"), with pointed average masses, are compared in the m/z range 2 to 20 KDa (a–c) and 17 to 90 KDa (e–g) with the spectra of LLC-MK2 uninfected cells (d,h). (i,j) Spectra view of the Average spectra profiles in the mass range 7,400–7,900 Da (i) and in the mass range 26,000 to 35,000 Da (j) of LLC-MK2 cells infected with the 3 different poliovirus serotypes with LLC-MK2 uninfected cells.

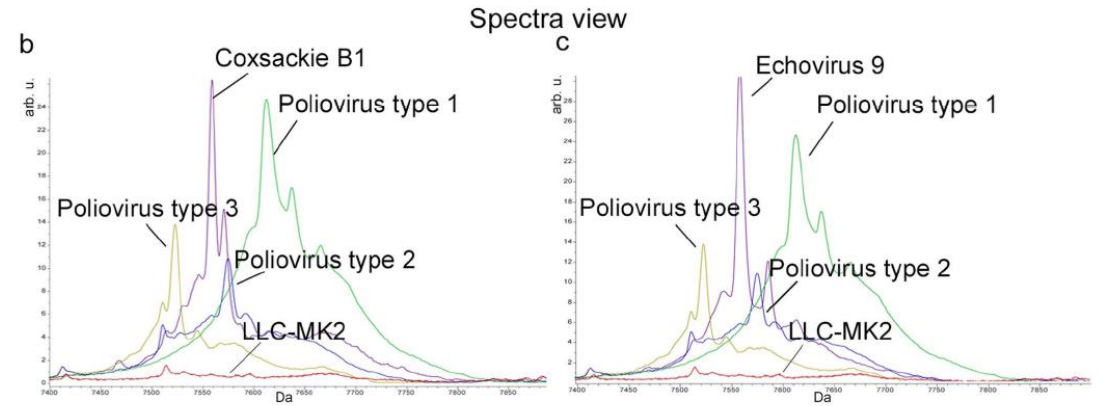

Figure 4 | Representative MALDI-TOF mass spectra of LLC-MK2 cells infected with the *Picornaviridae* family members human coxsackievirus B1 and human echovirus 9 and uninfected cells, and ClinPro Tools comparative analysis with the Sabin poliovirus type 1, 2, and 3 strains. (a) Spectra of LLC-MK2 cells infected with human coxsackievirus B1 and human echovirus 9 ("Coxsackie B1-infected cells" and "Echovirus 9-infected cells") compared with the protein profile of LLC-MK2 uninfected cells in the m/z range of 2 to 20 KDa. Molecular weight values are indicated on peak tops. (b,c) Spectra view of the average spectra of human coxsackievirus B1 (b) and human echovirus 9 (c) compared by ClinPro Tools in the mass range 7,400–7,900 Da with the average spectra of the 3 Sabin poliovirus strains (poliovirus type 1; poliovirus type 2; poliovirus type 3) and uninfected LLC-MK2 cells.

Calderaro A et al. Sci Rep 2014;4:6803.

TABLE I. Performance of matrix-assisted laser desorption ionization time-of-flight mass spectrometry (MALDI-TOF MS) identification with routine samples in clinical microbiology laboratories

Number of isolates tested	Manufacturer of the MALDI-TOF MS system	Overall correct identification at the species level (%)	Overall correct identification at the genus level (%)	Correct identification of Gram-negative bacteria at the species level (%)	Correct identification of Gram-positive bacteria at the species level (%)	References
1660[a]	Bruker Daltonics GmbH	84.1	11.3	NA	NA	[11]
1371[a]	Bruker Daltonics GmbH	91.7	2.8	88.8	88.0	[14]
720[a]	Bruker Daltonics GmbH	93.6	NA	98.2	83.9	[13]
720[a]	Shimadzu Corporation	88.3	NA	94.8	75.6	[13]
1116[b]	Bruker Daltonics GmbH	95.2	4.8	93.8	97.7	[10]

NA, not available.
[a]Prospective study.
[b]Retrospective study.

Bizzini A, Greub G. Clin Microbiol Infect 2010;16:1614.

TagIdent tool (formerly GuessProt)

TagIdent is a tool which allows

1. the generation of a list of proteins close to a given pI and Mw,
2. the identification of proteins by matching a short sequence tag of up to 6 amino acids against proteins in UniProtKB/Swiss-Prot close to a given pI and Mw,
3. the identification of proteins by their mass, if this mass has been determined by mass spectrometric techniques

for one or more species and with an optional keyword [references].

Documentation is available.

Fill out in the following form the *pI* (isoelectric point) and *Mw* (molecular weight) you wa
values in which the search should take place. Leave empty if you don't want to specify

The "Organism Name or Classfication or NCBI_TaxID" field allows you to specify terms
will only be returned, if all the given terms appear in either the *OS* or *OC* or *OX* lines of
particular be aware that if you enter "rat", all taxonomical terms containing the substring
even better its TaxID '10116') narrows down your search and probably corresponds bet

Scan in UniProtKB/Swiss-Prot can be restricted by the use of a keyword. This should b
keywords.

For example, entering the following values:

```
pI min = 5.15
```

Table 1. Peaks identified to separate the clusters.

Peak Position	Cluster 1	isolates 11 and 12	Cluster 2	Possible proteins (from TagIdent)
3444	Yes	Yes	No	Protamine-like protein
5873	Yes	Yes	No	Regulatory protein MokB
6539	Yes	No	No	50S ribosomal protein L30
7173	Yes	No	No	Pilin; Protein CopA/IncA
7650	No	No	Yes	Response regulator inhibitor for tor operon; Protein KleB; Protein IscX; Cold shock-like protein CspH
7708	Yes	Yes	No	Response regulator inhibitor for tor operon; Protein KleB; Protein IscX; Cold shock-like protein CspH
8326	Yes	Yes	No	Tautomerase PptA; Dihydrofolate reductase type 2; Ferrous iron transport protein A
8350	No	No	yes	Tautomerase PptA; Dihydrofolate reductase type 2; Ferrous iron transport protein A
9712	No	No	yes	30S ribosomal protein S17; Regulatory protein AriR; UPF0386 protein YjhX; Acid stress chaperone HdeA
9739	Yes	Yes	No	30S ribosomal protein S; Regulatory protein AriR 17; UPF0386 protein YjhX; Acid stress chaperone HdeA
10463	Yes	Yes	No	30S ribosomal protein S19; Sugar fermentation stimulation protein B
10489	No	No	Yes	30S ribosomal protein S19; Sugar fermentation stimulation protein B

doi:10.1371/journal.pone.0164260.t001

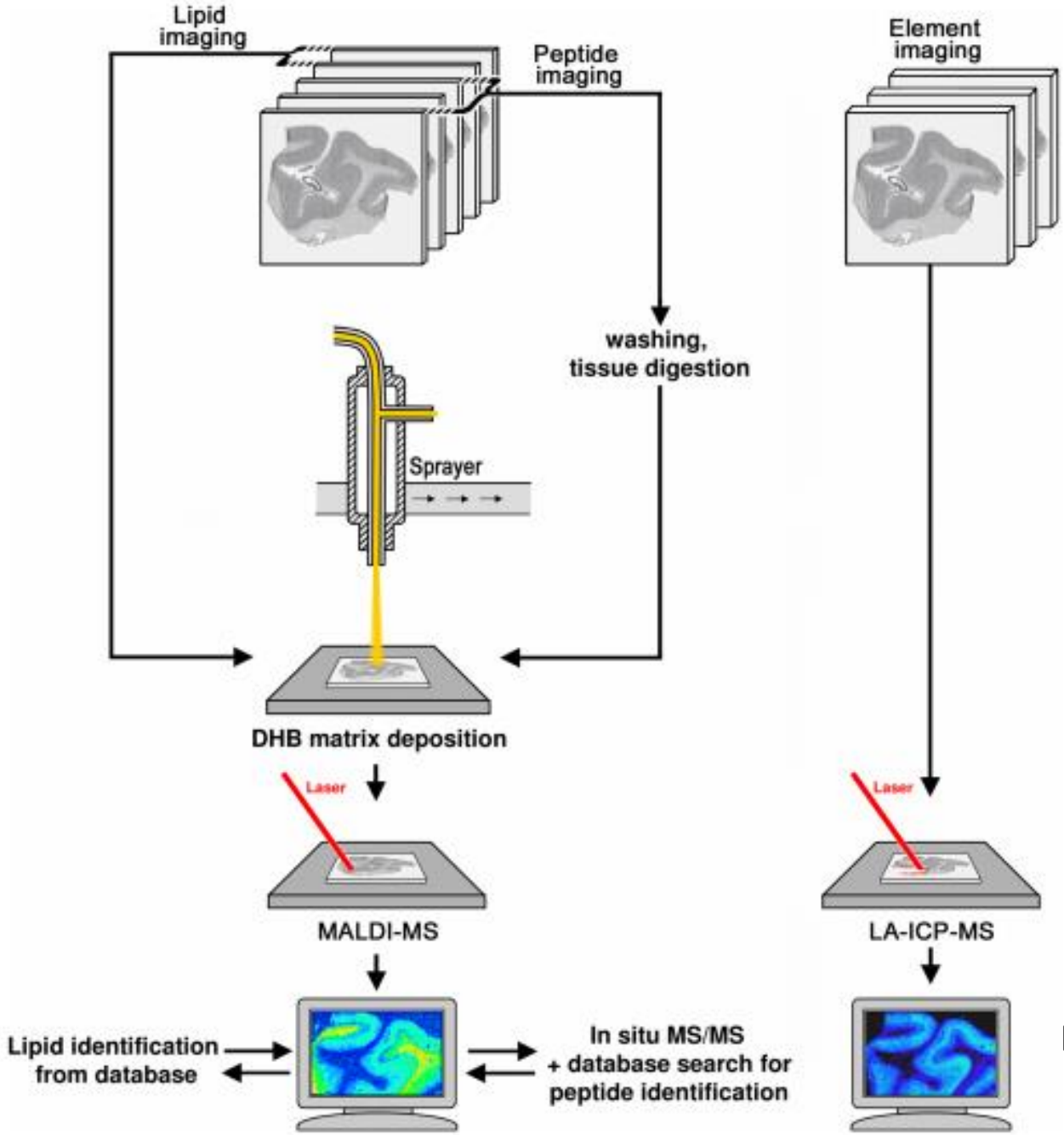

De San Román EG et al. Brain Struct Funct 2018;223:2767.

Fig. 5 Lipid distributions in the human primary visual cortex. **a** Myelin staining. **b** Nissl staining of sections adjacent to (**a**). **c**–**g** Lipid distribution images measured by MALDI-MSI tissue sections directly adjacent to the Nissl staining shown in (**b**). Images show the distributions of ions at **c** *m/z* 697.4787, identified as PA_34:1 + Na, **d** *m/z* 797.5919, identified as SM_d38:1 + K, **e** *m/z* 856.5848, identified as PC_40:6 + Na, **f** *m/z* 630.6181, identified as Cer_m40:0 + K and **g** *m/z* 768.5879, identified as PC_O-34:0 + H. Images were recorded in positive ion mode at 100 µm lateral resolution. Scale bar in **b** 5 mm, applies vertically to all images of the corresponding specimen. Color bars indicate normalized lipid ion intensities (arbitrary units, applies horizontally to the corresponding lipid across all specimens)

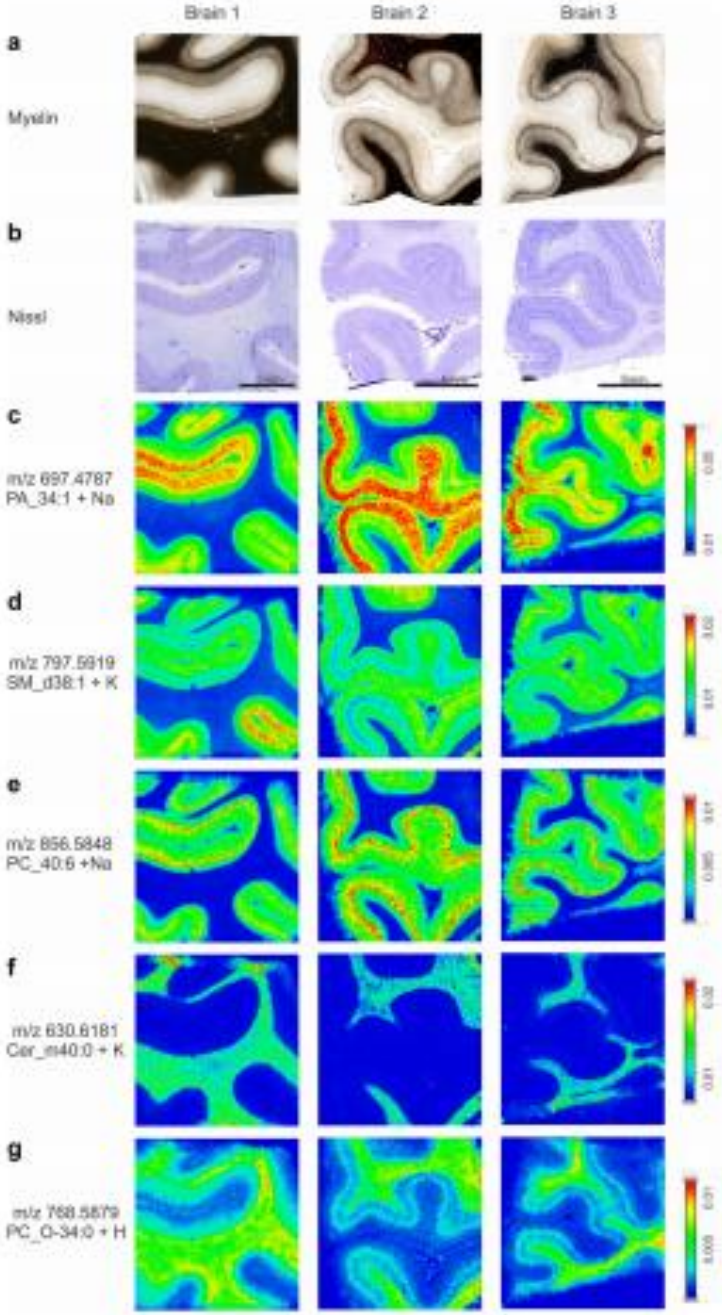

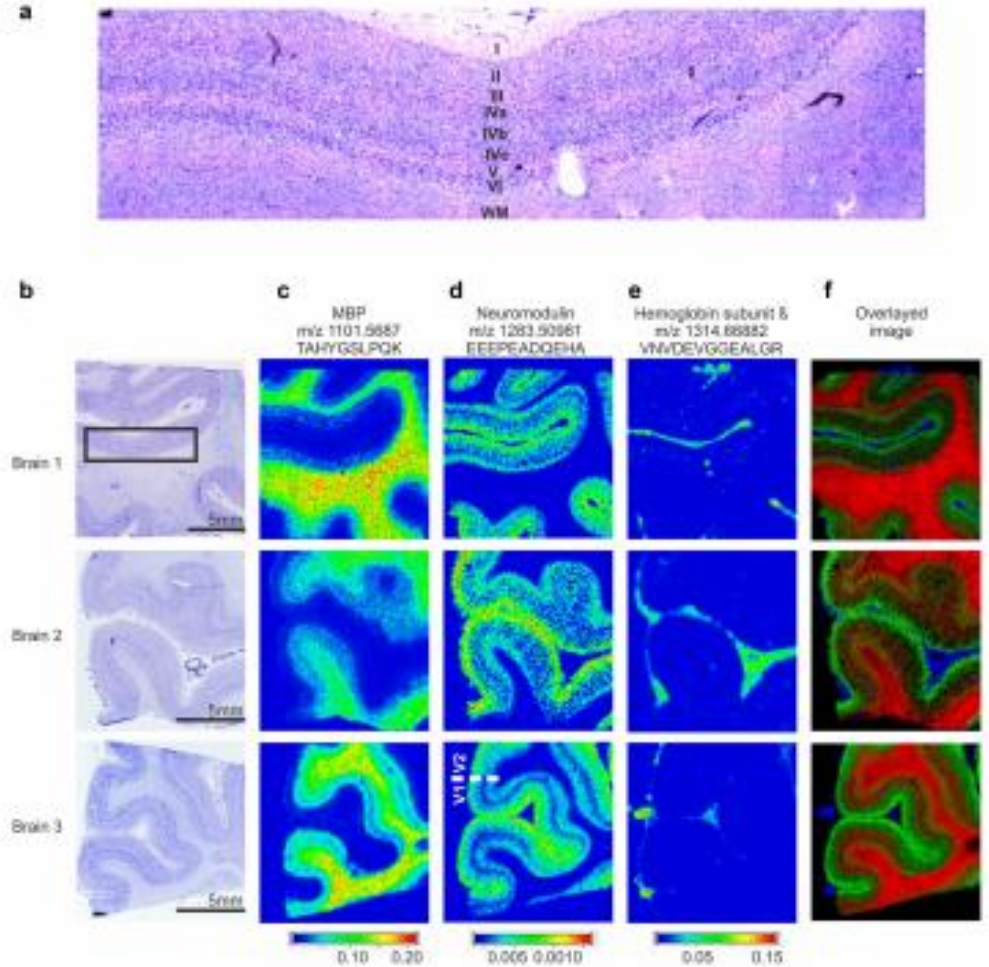

Fig. 2 Protein distributions in the human primary visual cortex determined by MALDI-MSI. **a** High-resolution image of a Nissl-stained section. Layer I, II, III, IVa–c, V, VI and white matter are indicated. **b** Nissl-stained sections from three different post-mortem brains. **c**–**e** Molecular feature images at **c** *m/z* 1101.5687, identified by MS/MS as a tryptic peptide of myelin basic protein, **d** *m/z* 1283.5998, identified as tryptic peptide of neuromodulin, **e** *m/z* 1314.6688, identified as tryptic peptide of hemoglobin β. **f** Overlay of the three peptide images highlighting their discrete distribution, MBP as red, neuromodulin as green and hemoglobin ß as blue. Spectra were recorded in positive ion mode at 100-µm lateral resolution. Black scale bar in panel **b**: 5 mm (applies horizontally to all images of the corresponding specimen). Color scales: Peptide ion intensity in arbitrary units (applies vertically to all images of the corresponding peptide)

adduct of ceramide (Cer)_m40:0, was enhanced along WM, but absent or reduced to non- detectable amounts in layer IVb (Fig. 5g). In contrast, the ion at *m/z* 768.5879, the protonated ion of PC_O-34:0, was abundant in WM including layer IVb (Fig. 5f). In summary, we were able to identify lipids specifically accumulating in different cortical layers and even sublayers of V1 or the WM.

To clarify if and how lipids differed between V1 and neighboring area V2, a tissue section containing the border between V1 and V2 was measured with the highest spatial resolution possible of 30 µm. Two lipid ions, the potassium

MALDI-Orbitrap MS

Orbitrap mass analyzer

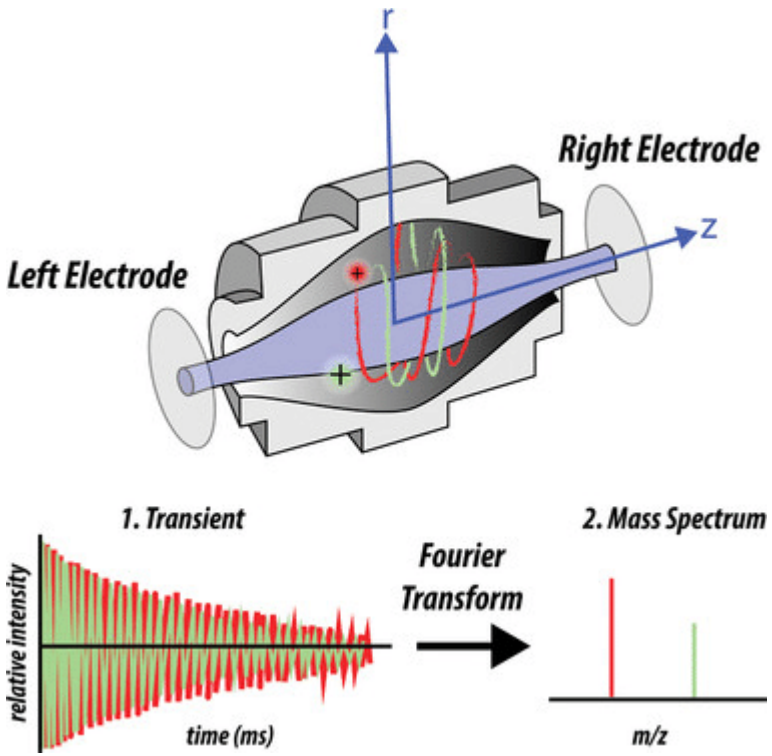

Savaryn JP et al. Proteomics 2016;16:2435.

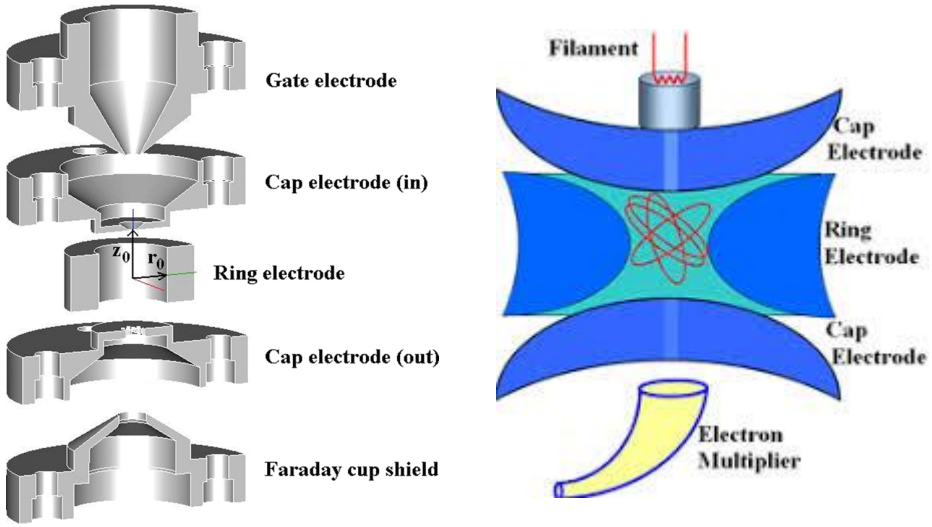

Ion trap mass analyzer

Concept of the Fourier transformation of time series data

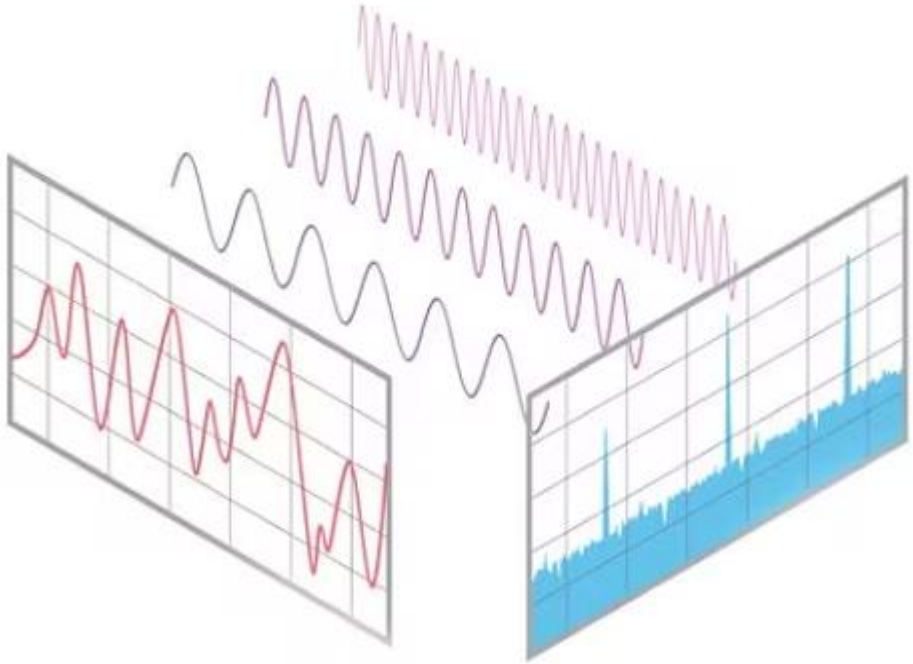

Orbitrap mass analyzer

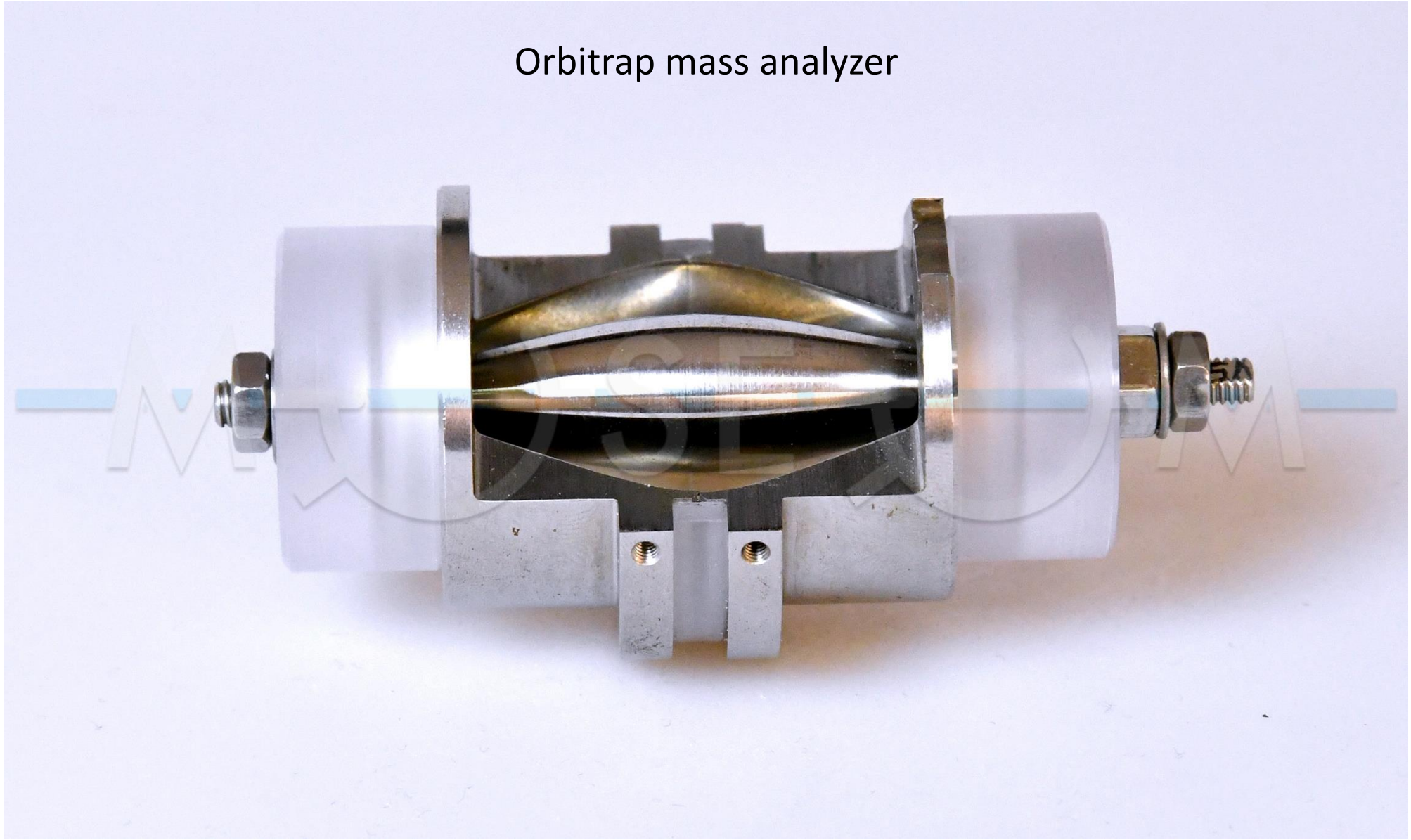

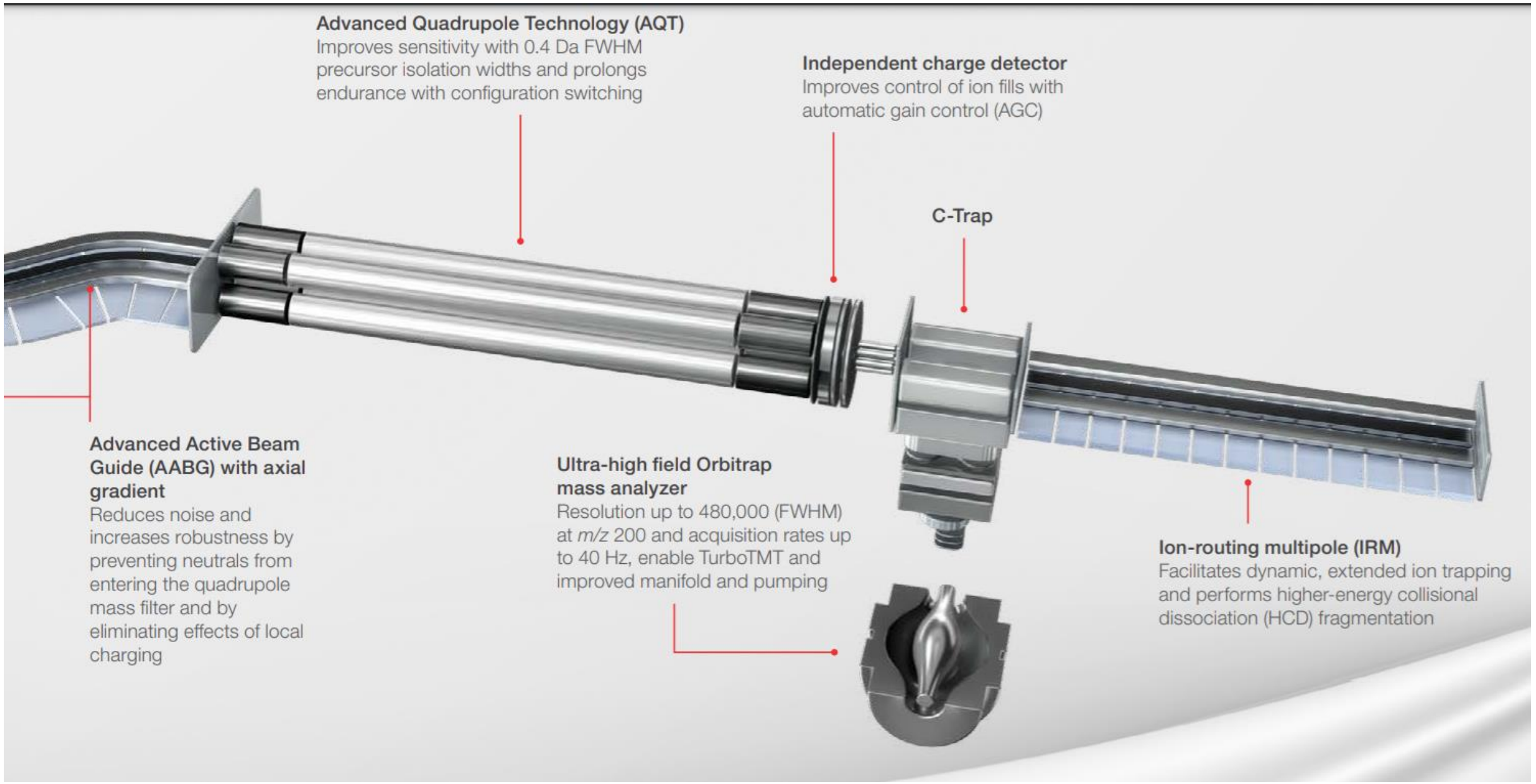

https://assets.thermofisher.com/TFS-Assets/CMD/brochures/br-65448-ms-orbitrap-exploris-480-br65448-en.pdf

https://www.youtube.com/watch?v=RsFsaCkVqxM